IEEE Access
Multidisciplinary | Rapid Review | Open Access Journal

Received January 18, 2021, accepted January 23, 2021, date of publication February 1, 2021, date of current version February 9, 2021.

Digital Object Identifier 10.1109/ACCESS.2021.3055774

Optimal Design of Passive Power Filter Using Multi-Objective Pareto-Based Firefly Algorithm and Analysis Under Background and Load-Side's Nonlinearity

MOHIT BAJAJ[1], (Member, IEEE), NAVEEN KUMAR SHARMA[2], (Member, IEEE), MUKESH PUSHKARNA[3], HASMAT MALIK[4], (Senior Member, IEEE), MAJED A. ALOTAIBI[5,6], (Member, IEEE), AND ABDULAZIZ ALMUTAIRI[7], (Member, IEEE)

[1]National Institute of Technology Delhi, New Delhi 110040, India
[2]Department of Electrical Engineering, I. K. Gujral Punjab Technical University, Jalandhar 144603, India
[3]Department of Electrical Engineering, GLA University Mathura, Mathura 281406, India
[4]BEARS, University Town, NUS Campus, Singapore 138602
[5]Department of Electrical Engineering, College of Engineering, King Saud University, Riyadh 11421, Saudi Arabia
[6]Saudi Electricity Company Chair in Power System Reliability and Security, King Saud University, Riyadh 11421, Saudi Arabia
[7]Department of Electrical Engineering, College of Engineering, Majmaah University, Al Majma'ah 11952, Saudi Arabia

Corresponding author: Hasmat Malik (hasmat.malik@gmail.com)

ABSTRACT In this paper, the optimal designing of passive power filter (PPF) is formulated as a multi-objective optimization (MOO) problem under several constraints of system's performance indices (PIs) such as individual as well as total harmonic distortion (THD) in the line current and the point of common coupling's (PCC) voltage, distribution line's ampacity under harmonic currents overloading, steady-state voltage profile, load power factor (PF) and a few associated with the filter itself. The optimal design parameters of a third-order damped filter are simultaneously determined for achieving maximum PF at the PCC while keeping system's other indices such as total demand distortion (TDD) in the line current, total voltage harmonic distortion (TVHD) at the PCC and total filter cost (FC) incurred at a minimum by obtaining a best-compromised solution using the newly proposed multi-objective Pareto-based firefly algorithm (pb-MOFA). A novel MOO approach inspired by the modified firefly algorithm and Pareto front is established in order to deal with PPF design problems. The extension of MOFA is considered for producing the Pareto optimal front and various conclusions are drawn by analysing the trade-offs among the objectives. The efficiency and accuracy of the proposed pb-MOFA, in solving the concerned MOO problem, is validated by comparing an obtained solution and three computed PIs viz. convergence metric (CM), generational distance (GD) and diversity metric (DM) with those obtained from popular multi-objective Pareto-based PSO (pb-MOPSO), non-dominated sorting genetic algorithm (NSGA-II) and recently introduced multi-objective slime mould algorithm (MOSMA). The need for true Pareto front (TPF) is served by the one obtained by Monte Carlo method. At last, the impacts of different background voltage distortion (BVD) levels and load-side's nonlinearity levels (NLLs) on filter performance are analysed.

INDEX TERMS Background distortion, firefly algorithm, harmonic compensation, harmonic distortion, multi-objective optimization, passive power filters.

ABBREVIATIONS

PPF	Passive Power Filter
MOO	Multi-Objective Optimization
PIs	Performance Indices
THD	Total Harmonic Distortion
PCC	Point of Common Coupling
PF	Power Factor
TDD	Total Demand Distortion
TVHD	Total Voltage Harmonic Distortion
FC	Filter Cost
pb-MOFA	Multi-Objective Pareto-Based Firefly Algorithm

The associate editor coordinating the review of this manuscript and approving it for publication was Dwarkadas Pralhaddas Kothari.

CM	Convergence Metric
GD	Generational Distance
DM	Diversity Metric
NSGA	non-dominated sorting genetic algorithm
MOSMA	multi-objective slime mould algorithm
TPF	True Pareto Front
BVD	Background Voltage Distortion
NLLs	Load-Side's Nonlinearity Levels
DNs	Distribution Networks
DNOs	Distribution Network Operators
RES	Renewable Energy Source
HC-HC	Harmonic-Constrained Hosting Capacity
APFs	Active Power Filters
HPFs	Hybrid Power Filters
VA	Voltage-Ampere
OFs	Objective Functions
HDF	Harmonic De-rating Factor
DHPF	Decoupled Harmonic Power Flow
ST	Single-Tuned
IC	Investment Cost
OC	Operating Cost
IHDV	Individual Order Harmonic Distortion in Voltage
IHDC	Individual Order Harmonic Distortion in Current

LIST OF SYMBOLS

$\bar{V}_S\,(1)$	Fundamental frequency component of voltage at the utility grid
$\bar{V}_S\,(h)$	The h^{th} order harmonic component of voltage at the utility grid
$A\,(h)$	A coefficient corresponding to background voltage
$\bar{Z}_L\,(h)$	Impedance offered by transmission line at h^{th} order harmonic frequency
$R_L\,(1)$	The resistance of the transmission line at the fundamental frequency
$X_L\,(1)$	The reactance of the transmission line at h^{th} order harmonic frequency
$R_L\,(h)$	The resistance of the transmission line at h^{th} order harmonic frequency
$X_L\,(h)$	The reactance of the transmission line at h^{th} order harmonic frequency
P_L	The active power consumption of the linear load
Q_L	The reactive power consumption of the linear load
$R'_L\,(h)$	The representative branch resistance of linear load at h^{th} order harmonic frequency
$X'_L\,(h)$	The representative branch reactance of linear load at h^{th} order harmonic frequency
$\bar{V}_L\,(1)$	The fundamental frequency component of voltage at the PCC
$\bar{V}_L\,(h)$	The h^{th} order harmonic component of voltage at the PCC
$Y'_L\,(h)$	The representative admittance of linear load at h^{th} order harmonic frequency
P_{NL}	The active power consumption of the nonlinear load
Q_{NL}	The reactive power consumption of the nonlinear load
$\bar{I}'_{NL}\,(1)$	The fundamental frequency component of current injected by the nonlinear load
$\bar{I}'_{NL}\,(h)$	The h^{th} order harmonic component of current injected by the nonlinear load
$C\,(h)$	A coefficient corresponding to the nonlinear load
S_d	The fundamental apparent power of DG unit
$\bar{I}_D\,(1)$	The fundamental frequency component of current injected by DG unit
$\bar{I}_D\,(h)$	The h^{th} order harmonic component of current injected by DG unit
$B\,(h)$	A coefficient corresponding to DG unit
K_n	The coefficient of nonlinearity level
ω_1	The fundamental frequency
R_f	Filter resistance
L_f	Filter inductance
C_1, C_2	Filter capacitances
$\bar{Z}_f\,(h)$	The equivalent net impedance of the filter circuit at h^{th} order harmonic frequency
$\bar{I}_L\,(h)$	The h^{th} order harmonic component of the line current
$\bar{I}_f\,(h)$	The h^{th} order harmonic component of the filter current
P_d	The total active power injection by the DG system
P_f	The fundamental power loss incurred in the filter
Q_f	The fundamental reactive power support capacity of the filter
K_1 to K_5	The cost weighting coefficients
OF_1 to OF_4	Objective functions
β	Distinctive attractiveness
β_0	Maximum attractiveness value
γ	Absorption coefficient
I	Light intensity of firefly
x_i^t	The position of a firefly at a specified time step t
rand	A random number between 0 and 1
g_*^t	The current best solution
w_k	A random number generated in each iteration
$\Psi\,(x)$	A combinatorial objective function
α_t	Randomness parameter
α_0	Initial random parameter

I. INTRODUCTION

It goes without saying that modern distribution networks (DNs) bear with high harmonic distortions owing to the amplified application of power electronics-based nonlinear load equipment and similar kind of practices are being

followed at each of the distribution power system buses, therefore, the idea of the linear distribution network is no longer a practical one. The high nonlinearity of loads throughout the DNs has led to a considerable distortion in all bus voltages and feeder currents due to aggregation of distortions of each bus with that of its background buses [1]. Additionally, under the presence of distributed generations the scenario in terms of harmonic distortions gets further exacerbated because of harmonic currents injected by DG units. Harmonic distortions are undeniably harmful to the DNs and the same fact is vindicated by life lessening of cables by harmonic derating, excessive transmission power loss, malfunctioning of consumer equipment and industrial drives and last but not the least communication interference [2], [3]. The standard indices, employed for quantifying total as well as individual order harmonic distortions in both PCC's voltage as well as line's current, must strictly follow IEEE Std. 519 and 1547 with as well as without the presence of DERs [4]–[6].

Moreover, even after being realistic for numerous applications, the required penetration potential of renewable energy has not been met yet crucially owing to the deteriorated harmonic performance of modern distribution networks (DNs) as well as several power quality issues associated with the DG units itself. Though the distribution network operators (DNOs) have negligible regulation over the location as well as renewable energy source (RES) type engaged in DG unit which is independently decided by DG owners yet the penetration level of renewable energy or technically speaking i.e. the size of DG unit is permitted to be extended only up to an extent where the system's harmonic distortion violates the associated international standard limit [7]. The penetration level of renewable energy at which any of the system's harmonic constraints starts getting violated is known as the harmonic-constrained hosting capacity (HC-HC) of the system [8], [9]. The poor harmonic performance of a distribution system also points out towards its poor capacity of hosting renewable energy.

A. MOTIVATION AND INCITEMENT

Among the abundant of way out and power conditioning devices that enhance the quality of power and alleviate harmonics passive power filters are most broadly employed in distribution power systems in order to compensate harmonic currents. Apart from the harmonic mitigation, PPFs offer reactive power support, which can improve the system power factor and thereby leading to reduce reactive power loss and enhanced voltage profile at the PCC [10]. At large, there exist three categories of power filters namely passive power filters [11], [12], active power filters (APFs) [13]–[15], and hybrid power filters (HPFs) [16]. Out of them, PPFs have been employed rather frequently than the other categories owing to their economic benefits, simplicity, stress-free surveillance and maintenance, and high reliability [17]. In its comprehensive prospect, PPFs are categorized based on the scheme of interconnection at PCC i.e. either into the series or shunt. Shunt PPFs are yet rather used for harmonics compensation than the series type PPFs due to the substantial fundamental power loss and voltage drop of series type PPFs, along with their relatively large fundamental voltage-ampere (VA) rating. Furthermore, shunt type PPFs are adept of supporting voltage and provide reactive power compensation at the fundamental frequency [18], [19].

Further, shunt type PPFs are categorized on the basis of their operation, into tuned and damped filters. Tuned filters are filters that are premeditated to mitigate harmonics by offering a low impedance path at one, two, or even three tuning harmonic frequencies, known as single-tuned, double-tuned, and triple-tuned (less common) filters, individually. Alternatively, tuned type PPFs labor under several downsides including parameter deviations that may happen owing to frequency deviation, manufacture filter tolerance, and temperature alteration. Also, the filtering performance is susceptible to the source resistance which may fluctuate and therefore leads to resonance occurrence between the filter and system [20], [21]. Oppositely, damped PPFs likewise the first-order, second-order, third-order, C-type, damped double-tuned, and band-pass filters, are high-pass filters that deliver a low impedance path to a wide range of harmonic frequencies. In distinction to the tuned PPFs, damped PPFs are less profound to deviations that may happen because of frequency deviation, manufacture tolerance, and temperature change. Similarly, damped PPFs can dampen the harmonic amplification which may take place through the resonance between the filter and the system.

B. LITERATURE REVIEW

In designing process of PPFs of any type, the researchers deal with the determination of the types, total numbers, values of the components and location in the concerned DN while setting some certain objectives such harmonic mitigation, reactive power compensation, voltage profile improvement etc. [12], [22], [23]. The designing of PPFs is a perplexing task owing to a great number of conflicting objectives in addition to a large number of nonlinear constraints being involved in the optimization process and also the optimal design on a PPF can't be obtained relying on the trial-and-error measures involved in the traditional methodologies [24]. In recent times, the expansion in nature-inspired metaheuristic optimization algorithms has given rise to new methods for designing the PPFs. Well prevalent PSO based algorithm has been developed in [25] for searching an optimal solution of planning of PPFs. Two objectives namely harmonic reduction and cost minimization are considered in the optimization process by amalgamating the two into a single one by the weighted sum method. Authors, in [26], proposed a PSO based approach with nonlinear time-varying evolution centered on a neural network where parameters are governed by employing a sequential neural network guesstimate. Nevertheless, PSO has comparatively fast convergence rate but again the overall fitness function is the linear weighted sum of all sub-OFs for formulating them into a single one. The renowned genetic algorithm (GA) is used in [27] for optimal

designing of PPF, though high computational burden and low convergence rate are two major shortcomings of GA. In [28], the usage of FORTRAN feasible sequential quadratic programming is revealed to obtain the optimal sizing of parameters of C-type PPFs for reducing the total voltage harmonic distortion of nonlinear loads, where retaining a specified PF at a particular range is anticipated. In [28] passive harmonic filters are designed for maximization of the loading capability of the transformers under non–sinusoidal environments. Moreover, for solving single-objective PPF optimization problem deterministic optimization methodologies such as deterministic sequential programming [29] and the golden section search method [30] are also applied in the literature. For the multi-objective approach, heuristic techniques, such as the hybrid differential evolution algorithm [31] and simulated annealing [32], are the utmost extensively applied methodology for finding the optimal parameters of filter.

C. PROBLEM FORMULATION

The abovementioned literature publications have made a substantial contribution to the problem of the optimal PPF design, along with illuminating several aspects of this subject. But still, the significant research gap is needed to be taken care of while designing any PPF for enhancing the PQ performance of a distribution system and motivates the authors to extend research contribution in the direction of passive power filter designing.

Plenty of algorithms undertook the optimal PPFs design as a single-objective optimization problem by formulating a combinatorial fitness function, by the linear weighted sum of all sub-objective functions, or attempted to transform a multi-objective problem into a single-objective one by allowing two or more objective functions (OFs) as ''acceptable level'' constraints [25]. Though, that practice usually results in an imbalance among the OFs and therefore get trapped in the local optimum. For dealing with such multi-objective problems it is always better to consider Pareto optimality and a set of feasible solutions called Pareto optimal set also called non-dominated solutions. By applying the concept of Pareto optimality, not only one but numerous solutions are acquired, which can assist a designer with a number of preferences to select a rather appropriate result. Besides that, most of the articles reported have assumed that the source voltage at the point of common coupling with the non-linear load is purely sinusoidal (i.e., free of harmonics) [25], [32]–[36]. For that reason, a further meticulous and organized exploration of this subject is desirable also if various BVD and NLL variations are envisioned to be taken into consideration.

D. CONTRIBUTION TO KNOWLEDGE

This paper formulates the optimal designing of PPF as a multi-objective optimization problem under several constraints of system's performance indices such as total demand distortion, total voltage harmonic distortion, load power factor, harmonic de-rating factor (HDF), individual order harmonic distortion in current and voltage, steady-state voltage profile and quite a few related with the filter itself. The optimization problem is formulated as simultaneously determining the accurate design parameters of a third-order damped filter at which PF at the PCC is maximum while system's other indices such as TDD, TVHD and total FC incurred are minimum by obtaining a best-compromised solution for the system. Incorporating the multiple objectives in filter designing problem can yield a rather win-win situation for the DN since a single compensating PPF offers multiple benefits. The multi-objective optimization problem of optimal PPF design has been dealt with by a newly proposed MOO approach inspired by the modified firefly algorithm and Pareto front. The extension of MOFA is considered for producing the Pareto optimal front and trade-offs among the objectives are analysed by plotting the same on different 2-axis planes. The efficiency and accuracy of the proposed pb-MOFA, in solving the concerned MOO problem, is validated by comparing an obtained solution and three computed PIs viz. convergence metric, generational distance and diversity metric with those obtained from popular multi-objective Pareto-based PSO [37], [38], non-dominated sorting genetic algorithm [39] and recently introduced multi-objective slime mould algorithm [40]. The Pareto front obtained from Monte Carlo method is nearly considered as the true Pareto front. The selection of the third-order damped filter is vindicated by its efficient performance due to reduced fundamental power losses [41], [42]. The system considered is a harmonically contaminated two bus distribution system while the same methodology can be applied to any distribution system with any number of buses. Initially, the studied base system is considered polluted with background nonlinearity, BVD $=$ 4.25% and NLL $=$ 40% and its performance enhancement is performed by the proposed approach. Thereafter, the impacts of different background voltage distortion levels, owing to nonlinearities present in the background, and different load-side's nonlinearity levels on filter performance are analysed.

E. PAPER ORGANIZATION

The remaining share of the article is arranged in the following fashion: After the introduction portion, the original research problem is formulated in section 2. Section 2 gives details on the system taken into consideration in the present study, mathematical modelling of the several components, power flow calculations. Formulation of the optimization problem with the comprehensive details on objective functions, associated constraints as well as algorithm applied is covered in a subsection of section 2 only. Section 3, firstly declares all the required numerical data of the system to be studied. Secondly, the filter is designed by the proposed methodology for meeting the required multi-objectives in the system. Section 4 infers the paper and recommends the directions for future research followed by the references listed in the end.

II. PROBLEM FORMULATION

The system taken into consideration for demonstration of the proposed approach is basically a typical two bus distribution

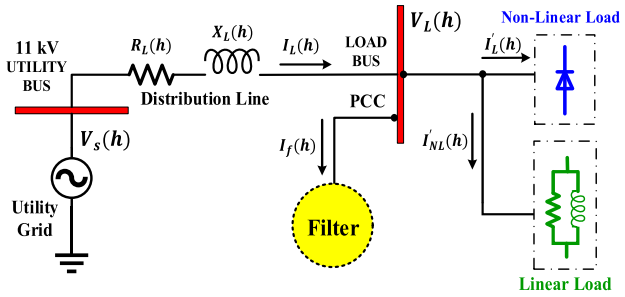

FIGURE 1. The configuration of the system under study.

system as depicted in figure 1 and has also been reported in many studies especially those focused on filter size optimization [19], [42], [43]. The load configuration is a hybrid type that is a combination of linear and nonlinear load which is assumed directly connected at PCC without secondary distribution transformer and feeder and entirely balanced also. The filter is as aforementioned a third-order damped type and its detailed modelling is given in the subsequent section.

A. MODELLING OF DIFFERENT COMPONENTS AND POWER FLOW CALCULATION

This work applies the decoupled harmonic power flow (DHPF) method for solving and computing various parameters of the system and the choice of the approach is vindicated by its simplicity of implementation and reduced computation burden. In the DHPF method, all order harmonics are decoupled and power flow calculation is separately performed for each of them instead of simultaneously. The system is firstly solved for voltage at PCC and line current at the fundamental frequency by applying nodal analysis at PCC in single-phase equivalent circuit shown in figure 3. After calculating the fundamental component of line current and voltage at PCC, the system is similarly solved for other harmonic frequencies.

The utility grid is considered as a slack or reference bus and h^{th} order harmonic component of the voltage at the slack bus is expressed as:

$$\bar{V}_S(h) = A(h) * \bar{V}_S(1) \tag{1}$$

where, $A(h)$ is a coefficient that depends on the level of the distortion in the background.

Impedance offered by transmission line at h^{th} order harmonic frequency, $\bar{Z}_L(h)$, is expressed as follows:

$$\bar{Z}_L(h) = R_L(h) + jX_L(h) = R_L(1).\sqrt{h} + jhX_L \tag{2}$$

where, $R_L(h)$ and $X_L(h)$ are the resistance and reactance of the transmission line at h^{th} order harmonic frequency while $R_L(1)$ and $X_L(1)$ are the resistance and reactance at the fundamental frequency. The resistance of transmission lines is assumed frequency-dependent due to eddy currents and the skin effect [44].

The linear load is modelled as a parallel combination of a resistor and an inductor in which resistor is accountable for active power consumption while inductor is assumed the one consuming reactive power as also depicted in the linear part of figure 1 and also in figure 3. If the active and reactive power consumption of linear load are P_{L} and Q_{L} respectively, the representative branch elements of linear load $R'_L(h)$ and $X'_L(h)$ at h^{th} order harmonic frequency are expressed as follows:

$$R'_L(h) = \frac{\left|\bar{V}_L(1)\right|^2}{P_L} \tag{3}$$

$$X'_L(h) = \frac{h\left|\bar{V}_L(1)\right|^2}{Q_L} \tag{4}$$

where, $\left|\bar{V}_L(1)\right|$ is the RMS of the fundamental frequency component of voltage at PCC. The admittance of linear load at h^{th} order harmonic frequency, $Y'_L(h)$, is expressed as follows:

$$Y'_L(h) = \left(\frac{P_L}{\left|\bar{V}_L(1)\right|^2} - j\frac{Q_L}{h\left|\bar{V}_L(1)\right|^2}\right) \tag{5}$$

The nonlinear load is modelled as a current source [45] and if the active and reactive power consumption of the nonlinear load is P_{NL} and Q_{NL} respectively, then the fundamental and h^{th} order harmonic component of current injected by the nonlinear load, $\bar{I}'_{NL}(1)$ and $\bar{I}'_{NL}(h)$ are expressed as follows:

$$\bar{I}'_{NL}(1) = \left(\frac{P_{NL} + jQ_{NL}}{\bar{V}_L(1)}\right)^* \tag{6}$$

$$\bar{I}'_{NL}(h) = C(h) * \bar{I}'_{NL}(1) \tag{7}$$

where, $C(h)$ is the ratio of h^{th} order harmonic component of current to the fundamental component and practically measured by performing field test and Fourier analysis of consumer load equipment.

The factor, K_{n} that defines the nonlinearity percentage or level (NLL) in the total load is expressed as follows:

$$K_n = \frac{P_{NL}}{P_L + P_{NL}} = \frac{Q_{NL}}{Q_L + Q_{NL}} \tag{8}$$

In present work, active and reactive power consumptions of linear as well as nonlinear load are selected on the basis of different nonlinearity levels for analysing its impact on filter's performance.

Figure 2 depicts the single-phase equivalent circuit of filter connected at PCC in figure 1 for h^{th} order harmonic frequency. It is a third-order damped filter that passes an extensive range of high-frequency harmonic currents to the ground. In this filter, a capacitor (C_2) is connected in series with the resistor (R_{f}). The reason for doing so is to considerably surge the impedance of the C_2 branch at the fundamental frequency compared to the inductive impedance provided by L_{f}. Such configuration will make the filter function as a single-tuned (ST) filter at low frequencies below the tuning one and therefore decrease the fundamental power loss. The capacitance value of the two capacitors can be chosen identical as well as different also depending upon the application. The equivalent

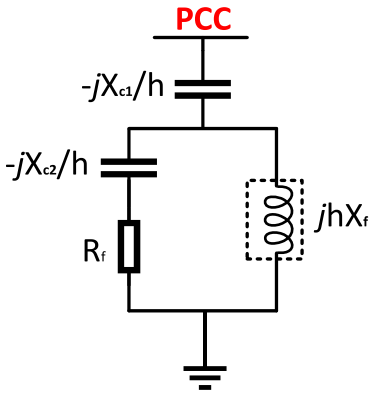

FIGURE 2. Single-phase equivalent circuit of third-order damped filter.

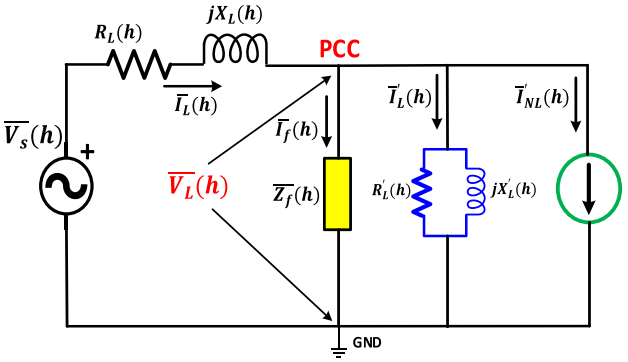

FIGURE 3. Single-phase equivalent circuit of the system under study.

net impedance of the filter circuit shown in figure 2 at h^{th} order harmonic frequency is expressed as:

$$\bar{Z}_f(h) = \frac{\alpha h^4 \omega_1^4}{h^2\omega_1^2(R_f C_2)^2 + \left(h^2\omega_1^2 L_f C_2 - 1\right)^2} + j\frac{\beta h^4\omega_1^4 + \gamma h^2\omega_1^2 - 1}{h\omega_1 C_1\left(h^2\omega_1^2(R_f C_2)^2 + \left(h^2\omega_1^2 L_f C_2 - 1\right)^2\right)} \tag{9}$$

In a third-order damped filter, one parameter is introduced as the characteristic harmonic order, h_n, given as follows:

$$h_n = \frac{1}{\omega_1 R_f C_1}$$

where, $\alpha = R_f L_f^2 C_2^2$, $\beta = R_f^2 C_2^2 L_f C_1 - L_f^2 C_1 C_2 - L_f^2 C_2^2$, $\gamma = L_f C_1 + 2L_f C_2 - R_f^2 C_2^2$ and $'\omega_1'$ is the fundamental frequency in rad/sec.

R_f: Filter resistance

L_f: Filter inductance

C_1, C_2: Filter capacitances

Figure 3 shows the overall single-phase equivalent circuit of the system under study and shown in figure 1.

Applying KCL at node-PCC in the circuit shown in figure 3, eq. (10) is obtained for h^{th} order harmonic frequency.

$$\bar{I}_L(h) = \bar{I}_f(h) + \bar{I}'_L(h) + \bar{I}'_{NL}(h) \tag{10}$$

where,

$$\bar{I}_L(h) = \frac{\bar{V}_S(h) - \bar{V}_L(h)}{R_L(h) + jX_L(h)} = \frac{A(h).\bar{V}_S(1) - \bar{V}_L(h)}{R_L(1).\sqrt{h} + jhX_L(1)} \tag{11}$$

Eq. (12) is the final eq. of the system in terms of unknown voltage variable $\bar{V}_L(h)$ at PCC for h^{th} order harmonic frequency. As aforementioned, eq. (12) is first solved for $h = 1$ i.e. at the fundamental frequency. Eq. (13) shows the eq. (12) at the fundamental frequency. Eq. (14) shows the expression of line current at a fundamental frequency while eq. (11) expresses the same for h^{th} order harmonic frequency. Thus following the steps of section 2.1, the entire system under study is solved.

$$\begin{aligned}\frac{A(h).\bar{V}_S(1) - \bar{V}_L(h)}{R_L(1).\sqrt{h} + jhX_L(1)} &= \frac{\bar{V}_L(h)}{\bar{Z}_f(h)} \\ &+ \bar{V}_L(h)\left(\frac{P_L}{|V_L(1)|^2} - j\frac{Q_L}{h\,|V_L(1)|^2}\right) \\ &+ C(h)\left(\frac{P_{NL} + jQ_{NL}}{\bar{V}_L(1)}\right)^*\end{aligned} \tag{12}$$

$$\begin{aligned}\frac{1\angle 0^\circ - \bar{V}_L(1)}{R_L(1) + jX_L(1)} &= \frac{\bar{V}_L(1)}{\bar{Z}_f(1)} + \bar{V}_L(1)\left(\frac{P_L}{|V_L(1)|^2} - j\frac{Q_L}{|V_L(1)|^2}\right) \\ &+ \left(\frac{P_{NL} + jQ_{NL}}{\bar{V}_L(1)}\right)^*\end{aligned} \tag{13}$$

$$\bar{I}_L(1) = \frac{1\angle 0^\circ - \bar{V}_L(1)}{R_L(1) + jX_L(1)} \tag{14}$$

where, $\left|\bar{V}_L(h)\right|$ is the RMS of h^{th} order harmonic component of the voltage at PCC

$\bar{I}_f(h)$ is the h^{th} order harmonic component of the filter current

$\bar{I}_L(h)$ is the h^{th} order harmonic component of the line current

B. FORMULATION OF THE OPTIMIZATION PROBLEM

As aforementioned also in the introduction section, the emphasis of the present work is on designing the third order high pass filter for achieving the maximum objectives usually concerned in passive filter planning. The optimization problem is formulated as to simultaneously setting the filter parameters as decision variables such that the multiple objectives such as minimum voltage THD, minimum current TDD, maximum PF and minimum filter cost are met all together. Numerous optimization models of passive as well active filters planning problem with multiple objectives are reported in the literature [46], [47] and the common objectives have been voltage THD and current TDD reduction, PF improvement and cost optimization etc. The detailed coverage on

objective functions, constraints and algorithm employed for optimization purpose is as follows:

1) OBJECTIVE FUNCTION

The objective function used in this work is composed of four objective functions that are required to be minimized as expressed by eq. (15):

$$\text{Min } OF = [OF_1, OF_2, OF_3, OF_4] \tag{15}$$

The first objective function (OF_1) is the minimization of TDD in the line current as expressed by eq. (16),

$$OF_1 = \text{Min } TDD\left(R_f, L_f, C_1, C_2\right) \tag{16}$$

Total demand distortion (TDD) is an index used for quantifying the harmonic performance of transmission cable with and without the DGs. IEEE Std. 519 limits allowable TDD in the system depending upon the maximum demand load current (I_{mL}), fault level and the kind of DG system such as dispersed generation, utility distribution generating equipment or as a customer [48]. TDD (%) is formulated as per eq. (17).

$$TDD(\%) = \frac{\sqrt{\sum_{h=2}^{n} \left|\bar{I}_L\left(h\right)\right|^2}}{I_{mL}} * 100 \tag{17}$$

The second objective function (OF_2) is the minimization of THD in voltage at PCC as expressed in eq. (18)

$$OF_2 = \text{Min } THVD\left(R_f, L_f, C_1, C_2\right) \tag{18}$$

Total voltage harmonic distortion is formulated as per eq. (19)

$$TVHD\left(\%\right) = \frac{\sqrt{\sum_{h=2}^{n} \left|\bar{V}_L\left(h\right)\right|^2}}{\left|\bar{V}_L\left(1\right)\right|} * 100 \tag{19}$$

The third objective function (OF_3) is the maximization of overall PF at PCC as expressed in eq. (20)

$$OF_3 = \text{Max } PF\left(R_f, L_f, C_1, C_2\right) \tag{20}$$

Though, the overall optimization is performed as a minimization problem hence final OF_3 is expressed by eq. (21).

$$OF_3 = \text{Min}\left\{1 - PF\left(R_f, L_f, C_1, C_2\right)\right\} \tag{21}$$

Maximization of PF is no doubt vindicated by line loss reduction due to reduced reactive power flowing through it. Under a distorted environment, PF is calculated from eq. (22).

$$PF = \frac{\sum_{h=1}^{n} \left|\bar{V}_L\left(h\right)\right| . \left|\bar{I}_L\left(h\right)\right| . \cos\theta_h}{\sqrt{\sum_{h=1}^{n} \left|\bar{V}_L\left(h\right)\right|^2} . \sqrt{\sum_{h=1}^{n} \left|\bar{I}_L\left(h\right)\right|^2}} \tag{22}$$

The fourth and last objective function (OF_4) is the minimization of overall filter cost as expressed in eq. (23).

$$OF_4 = \text{Min } FC\left(R_f, L_f, C_1, C_2\right) \tag{23}$$

For taking the overall economic aspect of the filter into consideration, both investment cost (IC), as well as operating cost (OC), are considered. The investment cost is determined by values of individual elements such as resistor, inductor and capacitors and fundamental reactive power support capacity of the filter [42], [49]. Whereas the operating cost depends on fundamental real power loss incurred during the operation. Therefore, overall FC is computed by a linear sum of each element value, the capacity of the filter (in KVAr) and power loss (in kW) as shown in Eq. (24).

$$FC = \left\{K_1 R_f + K_2 L_f + K_3\left(C_1 + C_2\right) + K_4 P_f\right\}_{IC} + \left(K_5 Q_f\right)_{OC} \tag{24}$$

where P_f and Q_f are fundamental power loss and reactive power support respectively, K_1 to K_5 are cost weighting coefficients in pu/Ω, pu/mH, pu/μF, pu/kW and pu/KVAr respectively. The value of these coefficients is taken from reference [49] and mentioned in the subsequent section of results and discussion.

2) OPTIMIZATION CONSTRAINTS

Due to several limits on the choice of control variables in the practical applications, the objective function is subjected to several constraints as follows:

a: TOTAL HARMONIC DISTORTION

Total voltage harmonic distortion (%) at PCC is considered to be constrained under well-known max. allowable limit of 5% as per IEEE Std. 519 [5] without and also under the presence of integrated distributed generation systems and expressed as per eq. (25). IEEE Std. 519 limits allowable TDD in the system depending upon the maximum demand load current (I_{mL}), fault level and the kind of DG system such as dispersed generation, utility distribution generating equipment or as a customer [48]. TDD (%) is assumed to be constrained as per eq. (26).

$$TVHD\left(R_f, L_f, C_1, C_2\right) \leq 5\% \tag{25}$$

$$TDD\left(R_f, L_f, C_1, C_2\right) \leq 8\% \tag{26}$$

b: INDIVIDUAL ORDER HARMONIC DISTORTION

IEEE Std. 519 bounds the RMS of every order harmonic component of voltage at PCC and line current in percent to the fundamental component. Eq. (27) expresses the constraint of individual order harmonic distortion in voltage (IHDV) which is bound to 3% for components of all orders at an operating voltage below 69 kV. The individual order harmonic distortion in the current (IHDC) is constrained to different values depending on the harmonic order. Table 1 shows the maximum allowed IHDC for harmonics of all orders as per IEEE Std. 519. Though the even-order harmonics are allowed to 25% of odd-order harmonics limits according to IEEE Std. 519 and the same criteria are considered in this work yet the logic behind the idea of 25% is still vague and the authors of this paper believe that allowable limits on even and odd-order harmonics should be identical because of negligible energy and hence PQ issues associated with them.

$$\%IHDV\left(R_f, L_f, C_1, C_2\right) = \left(\frac{\left|\bar{V}_L\left(h\right)\right|}{\left|\bar{V}_L\left(1\right)\right|}\right)_{h>1} \leq 3\% \tag{27}$$

TABLE 1. Maximum permissible IHDC as per ieee std. 519.

Harmonic order	$IHDC_{\max}$
h<11	7
11≤h<17	3.5
17≤h<23	2.5
23≤h<35	1
35≤h	0.5

$$\%IHDC\left(R_f, L_f, C_1, C_2\right) = \left(\frac{\left|\bar{I}_L\left(h\right)\right|}{\left|\bar{I}_L\left(1\right)\right|}\right)_{h>1} \leq IHDC_{max} \tag{28}$$

c: POWER FACTOR

Power factor at the PCC is subjected to following nonlinear inequality constraint. PF is computed from Eq. (22) and the criteria are selected as per ref. [12], [19], [43]:

$$0.9 \leq PF\left(R_f, L_f, C_1, C_2\right) \leq 1.0 \tag{29}$$

d: LINE LOADING CAPABILITY

An index called harmonic de-rating factor is used for quantifying the overloading of transmission line in the harmonic distorted environment and the same is formulated and constrained by eq. (30) [50].

$$\%HDF\left(R_f, L_f, C_1, C_2\right) = \frac{1}{\sqrt{1+\sum_{h=2}^{n}\left(\frac{R_L(h)}{R_L(1)}\right)\left(\frac{\left|\bar{I}_L(h)\right|}{\left|\bar{I}_L(1)\right|}\right)^2}} * 100 \leq 100 \tag{30}$$

e: BUS VOLTAGE LIMITS

Entirely during the optimization overall RMS of voltage at PCC is bound to sustain under the lower limit of 0.95 pu and upper limit of 1.05 pu. Overall RMS of voltage is computed and constrained as per eq. (31).

$$0.95 \leq V_L\left(rms\right) = \sqrt{\sum_{h=1}^{n}\left|\bar{V}_L\left(h\right)\right|^2} \leq 1.05 \tag{31}$$

f: FILTER DESIGN CONSTRAINTS

Equations (32) and (33) facts out two constraints; the first one is the lowest boundary of C_2, and the second one is the range of the damping resistance R_f, its minimum value is given as $\left(2L_f/C_1\right)^{0.5}$, and the inverse relationship between R_f and C_2 as the minimum value of R_f occurs at the maximum value of C_2, at $C_2 = C_1$ [51]. The chief requirement of the auxiliary capacitor in the third-order damped filter is to lessen the filter loss at the fundamental frequency. It is, consequently, reasonable to employ loss minimization to establish the constraint specified by (32) [52]. Damping constant ratio m is defined and constrained as per equation (34).

$$\frac{C_1 L_f}{R_f^2 C_1 - L_f} \leq C_2 \leq C_1 \tag{32}$$

$$R_f \geq \sqrt{\frac{2L_f}{C_1}} \tag{33}$$

$$m = \frac{L_f}{R_f^2 C_1} \leq 1 \tag{34}$$

g: DECISION VARIABLE CONSTRAINTS

The five decision variables in the optimization process are manipulated as always constrained to exist between particular bounds as follows:

$$0.0 \leq R_f \leq 10.0 \tag{35}$$

$$0.0 \leq L_f \leq 10.0 \tag{36}$$

$$0.0 \leq (C_1, C_2) \leq 200.0 \tag{37}$$

3) FIREFLY ALGORITHM BASED SOLUTION OF OPTIMIZATION PROBLEM

For solving the formulated multi-objective optimization problem, firefly algorithm is applied in this work. FA is a metaheuristic and swarms intelligence based optimization approach that works on the concept of flashing behaviour of fireflies [53]. Though the FA has many likenesses with other nature-inspired algorithms yet according to the literature FA attains the capability of outperforming many other commonly used algorithms for example PSO and GA and the same has been validated by the statistical performance of FA in solving an optimization problem using standard stochastic test functions in several areas [54]. The basic reason lies in using real random numbers and global communication among the fireflies. Authors in [55] validated by numerous test functions that PSO repeatedly outperforms traditional algorithms like genetic algorithms in finding the global optima while the FA is superior to both PSO and GA in terms of both efficiency and success rate. Metaheuristic algorithms such as PSO and GA have found their extensive application in solving optimization problems governing the planning of distributed generation [56], passive filters and many more power quality enhancement devices nevertheless references [57]–[59] have reported the optimization efficiency of FA being rather superior than GA and PSO in single-objective problems of DG planning. Owing to the success achieved by the FA in several other engineering applications, their extension to the multi-objective context of power system planning with making good trade-offs among the objectives is quite desirable. FA is based on the formula of light intensity I that drops with the surge in the square of the distance r^2. The phenomena of decrement in light intensity due to its weakening by light absorption with increase in distance from light source is related with the mixed objective function to be minimized. FA implementation is inspired from three basic characteristics of fireflies as follows:

- All fireflies are unisex, and they will move towards more attractive and brighter ones regardless of their sex.
- Attractiveness is proportional to their brightness, thus for any two flashing fireflies, the less bright one will move towards the brighter one.
- The light intensity of a firefly is affected or determined by the landscape of the fitness function.

Each of the fireflies has its distinctive attractiveness β which infers towards how powerfully it attracts other fireflies of the swarm population. Since the firefly attractiveness, a monotonically decreasing function of the distance $r_j = d(x_i, x_j)$ should be considered for the selected firefly j, that is the following exponential function:

$$\beta = \beta_0 e^{-\gamma r_j} \tag{38}$$

where, β_0 and γ are two pre-specified parameters of algorithm i.e. maximum attractiveness value and absorption coefficient, respectively. Moreover, every particle of the population is characterized by its light intensity I_i which can be directly expressed as an inverse of a fitness function $f(x_i)$. Thus moving at a specified time step t of a firefly i toward a better firefly j is defined as:

$$x_i^t = x_i^{t-1} + \beta\left(x_j^{t-1} - x_i^{t-1}\right) + \alpha\left(rand - \frac{1}{2}\right) \tag{39}$$

where the term $\beta\left(x_j^{t-1} - x_i^{t-1}\right)$ adds the factor of attractiveness, β, while the term $\alpha\left(rand - \frac{1}{2}\right)$ which is controlled by the parameter α, is accountable for adding certain randomness in the path followed by the firefly, and *rand* is a random number between 0 and 1.

In a multi-objective optimization problem, the total number of OFs to be minimized are somewhat larger and all are intended to be minimized simultaneously. However, owing to the conflicts among the objectives, expecting the simultaneous minimization of all become quixotic. One possible of handling the multiple objectives is to form a combinatorial objective function by the linear weighted sum of all sub-objective functions. Nevertheless, that practice generally leads to an imbalance among the OFs and therefore get trapped in the local optimum. For dealing with such multi-objective problems it is always better to consider Pareto optimality. By considering the aforementioned basic idea of FA the pseudo-code of multi-objective FA can be framed as depicted in table 2 [60].

Initially, all the objective functions are defined approximately along with the associated constraints and the vector of search variables. Afterwards, the entire population of fireflies is initiated and made to get uniformly distributed among the search space where sampling techniques plays a crucial role. Now the iteration starts and brightness of fireflies or values of OFs are assessed and pairwise comparison is made. At that time, an arbitrary weight vector is produced (with the sum equal to 1), so that the overall best of each of the fireflies g_*^t can be guessed. The non-dominated solutions are then passed onto the next iteration. After executing the entire iterations all non-dominated solution points (equal to the total population considered) are used to estimate the true Pareto front.

TABLE 2. Pseudo Code: multi-objective firefly algorithm (MOFA).

Define objective functions $f_1(\boldsymbol{x}),\ldots\ldots\ldots, f_K(\boldsymbol{x})$ where $\boldsymbol{x} = (x_1, \ldots\ldots\ldots, x_d)^T$
Initialize a population of n fireflies $\boldsymbol{x}_i$ $(i = 1,2, \ldots\ldots\ldots, n)$
while (t < MaxGeneration)
quad **for** $i, j = 1: n$ (all n fireflies)
Evaluate their approximations PF_i and PF_j to the Pareto front
if i ≠ j and when all the constraints are satisfied
if PF_j dominates PF_i,
Move firefly i towards j using (39)
Generate new ones if the moves do not satisfy all the constraints
end if
if no non-dominated solutions can be found
Generate random weights w_k $(k = 1,2, \ldots\ldots\ldots, K)$
Find the best solution g_*^t (among all fireflies) to minimize Ψ in (40)
Random walk around g_*^t by (41)
end if
Update and pass the non-dominated solutions to next iterations
end
Sort and find the current best approximation to the Pareto front
Update $t = t + 1$
end while
Postprocess results and visualisation;

So as to do random walks rather competently, the current best g_*^t which minimizes a combinatorial objective can be found via the weighted sum as expressed in eq. (40). Where w_k is a random number, generated in each iteration according to the uniform distribution. The best value of $\Psi(x)$ for each iteration is called g_*^t.

$$\Psi(x) = \sum_{k=1}^{K} w_k f_k, \sum_{k=1}^{K} w_k = 1 \tag{40}$$

In case of one firefly dominating another, eq. (41) is applied to the moving fireflies. If a firefly is not dominated by others, the firefly is moved:

$$x_i^{t+1} = x_i^t + g_*^t \alpha_t \tag{41}$$

In eq. (41) g_*^t denotes to the best solution obtained for a particular set of random weights. The randomness parameter α_t is reduced for each iteration as $\alpha_t = \alpha_0 0.9^t$ where α_0 is the initial random parameter.

For multi-objective minimization problems, a solution vector $\boldsymbol{u} = (u_1, \ldots\ldots\ldots, u_n)^T$ is called dominating another vector $\boldsymbol{v} = (v_1, \ldots\ldots\ldots, v_n)^T$ if and only if $u_i \leq v_i$ for $\forall i \in \{1, \ldots, n$ and $\exists i \in \{1, \ldots, n\} : u_i \leq v_i$. It can be simply said that at least one element of u should be smaller than v.

The computational complexity, involved for evolving a single generation of the population, is $O(n_o n_p^2)$, where n_o is the number of objectives and n_p is the population size.

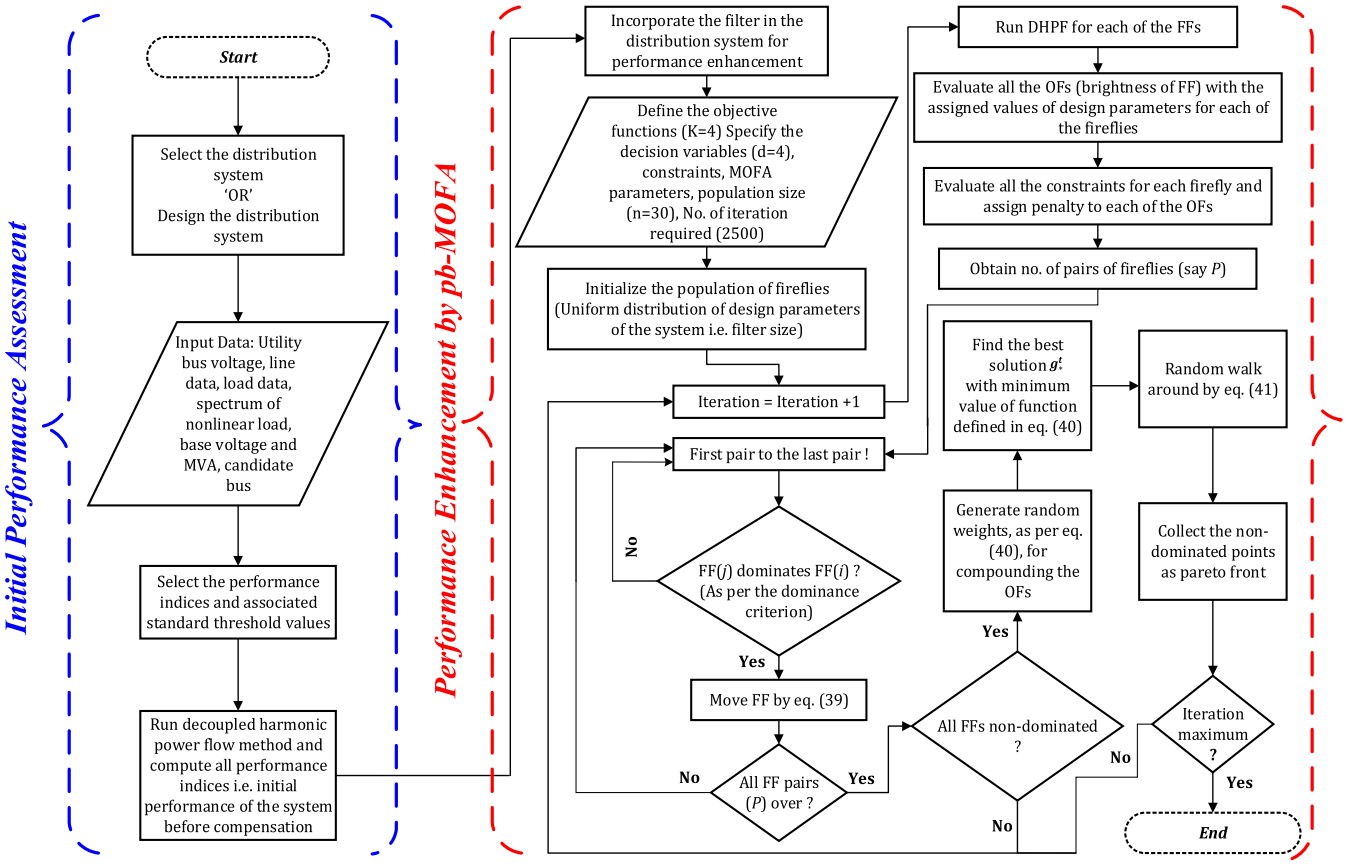

FIGURE 4. The overall flowchart of the proposed passive filter design approach by pb-MOFA.

However, for computing the aggregate complexity of the proposed pb-MOFA algorithm, it is mandatory to know both the complexity for each generation and the number of generations. Hence we can say that the actual complexity is $O(n_g n_o n_p^2)$, where $n_g$is the number of generations. According to the stopping criteria involved, n_g can have any complexity from constant to the upper bound.

Figure 4 depicts the overall flowchart of the proposed passive filter design approach by pb-MOFA. The procedure starts with an initial performance assessment of the distribution system under consideration. After reading the entire technical configuration, the initial performance of the uncompensated system is first evaluated by applying the DHPF at the candidate bus. Moreover, after performing the initial assessment it must be analysed whether the performance of the system under consideration comply with IEEE standard 519 for distortion in PCC voltage and line current or not. Normally the systems under deliberation need initial assessment owing to the severe distortions in voltage as well as the current which is further present due to high nonlinearity level present in the load. Violation of harmonic tolerances specified by the international standards automatically makes distribution network buses qualified for the auxiliary compensators. Subsequent to the initial performance assessment the main role of the proposed approach comes in. Irrespective of the performance of the system before the compensation, the filter is incorporated into the DHPF of the system. The total number of objectives as well as decision variables are four as also specified in the previous section. The whole population of fireflies is uniformly initialised with filter parameters. The envisioned OFs and constraints are evaluated by running the DHPF for each FF. Penalties are equally applied to each of the computed OFs for the constraint violations. The brightness of FFs is compared (criterion of dominance) for gathering the non-dominated FFs. At each iteration, the new position of a FF is compared with its current personal best g_*^t. In case both are reciprocally non-dominated, random selection is taken. At the end of each iteration, all the non-dominated points correspond to the Pareto front. The optimization process is repeated multiple times with a large number of firefly population as well as iterations in each cycle so that a large number of Pareto front, corresponding to multiple OFs, can be collected. All the non-dominated individuals are represented in the 2-axis planes and trade-offs among the planned objectives are analysed.

III. RESULTS AND DISCUSSION

The present section firstly declares all the required numerical data of the system to be considered and also shown in figure 1. Following the same, initial DHPF is performed on the system so as to identify the background performance of the system

TABLE 3. Harmonic contents of nonlinear load's current as a percentage of its fundamental current.

Harmonic Order	Magnitude (%)	Harmonic Order	Magnitude (%)	Harmonic Order	Magnitude (%)
3	15	19	5.3	35	2.4
5	12	21	4.7	37	2.2
7	11	23	4.3	39	2.0
9	8.1	25	4.0	41	1.8
11	7.1	27	3.7	43	1.6
13	6.4	29	3.4	45	1.4
15	5.8	31	2.8	47	1.3
17	5.5	33	2.6	49	1.2

TABLE 4. The spectrum of considered background voltage distortion.

Harmonic order (odd harmonics)						
h<7	7≤h<13	13≤h<25	25≤h<35	35≤h<45	45≤h≤49	BVD(%)
0.40	0.30	0.20	0.10	0.05	0.05	1
2.00	1.25	0.80	0.50	0.25	0.15	4.25

and thereby deciding the requisite of applying passive filter compensation. Secondly, the filter is designed by the proposed methodology for meeting the required multi-objectives in the system.

Referring to figure 1, utility gird is assumed operating at three balance voltage of 11 kV at the fundamental frequency i.e. $\left|\bar{V}_S\,(1)\right|$. Distribution line is assumed fully transposed and overall resistance and reactance of the same, at the fundamental frequency, i.e. $R_L\,(1)$ and $X_L\,(1)$ are 0.455 Ω and 1.165 Ω respectively. Voltage and current ratings of the distribution line are 11 kV and 525 A respectively. The base voltage of 11 kV and base MVA of 10 MVA is used for transforming all the quantities into their respective per unit. Maximum demand load current (I_{mL}) is calculatedly selected identical to the rated current carrying capacity of the line. The nonlinear load is SMPS type which injects all the odd-order harmonics into the system parting the usual exclusion of triplen harmonics [61], [62]. The harmonic spectrum of the nonlinear load is depicted in table 3. Only magnitude column is present and angle column is skipped in both table 3 owing to the angle is zero for each harmonic frequency. The maximum allowable limit in individual order harmonic distortion in both current and voltage is opted as per the IEEE Std. 519 [5] and previously mentioned in table 1 and eq. (27). The same Std. restricts the acceptable limits of TDD and TVHD at 8% and 5% respectively. Harmonics up to 49th order are considered for analysis purpose. Total active power consumption by the hybrid load is 7.2 MW while total reactive power consumption is 3.8 MVAr and the total value of both is kept constant in each scenario. NLL is considered 40% which means active and reactive power consumption by the linear load are 4.32 MW and 2.28 MVAR respectively and active and reactive power consumption by the nonlinear load are 2.88 MW and 1.52 MVAR respectively. The presence of BVD is initially neglected and considered in extended analysis. The percentage BVD of 4.25% is initially considered in analysis. The spectrum of considered background voltage distortion is shown in table 4.

TABLE 5. Background performance of the distribution system without compensation.

Parameter	Value
Voltage at the PCC (pu)	0.9329
HDF of the distribution line (%)	99.06
TVHD at the PCC (%)	8.25
TDD of the line current (%)	7.46
PF at the PCC	0.8775
Transmission losses (kW)	293.81

After running the DHPF in the distribution system without filter compensation, the background level of performance indices is obtained as shown in table 5. Performance in terms of individual order harmonic distortion, present in PCC voltage and line current, is represented by the radar chart depicted in figure 5. Figure 5 contains only odd-order harmonics since even order harmonics are absent owing to their absence in the load spectrum as well as background. A bird's eye view of system parameters depicted in table 5, in addition to figure 5, suggests that individual order harmonic distortion, in both current and voltage, is under the maximum tolerable limit stated by IEEE Std. 519 while TVHD exceeds the threshold

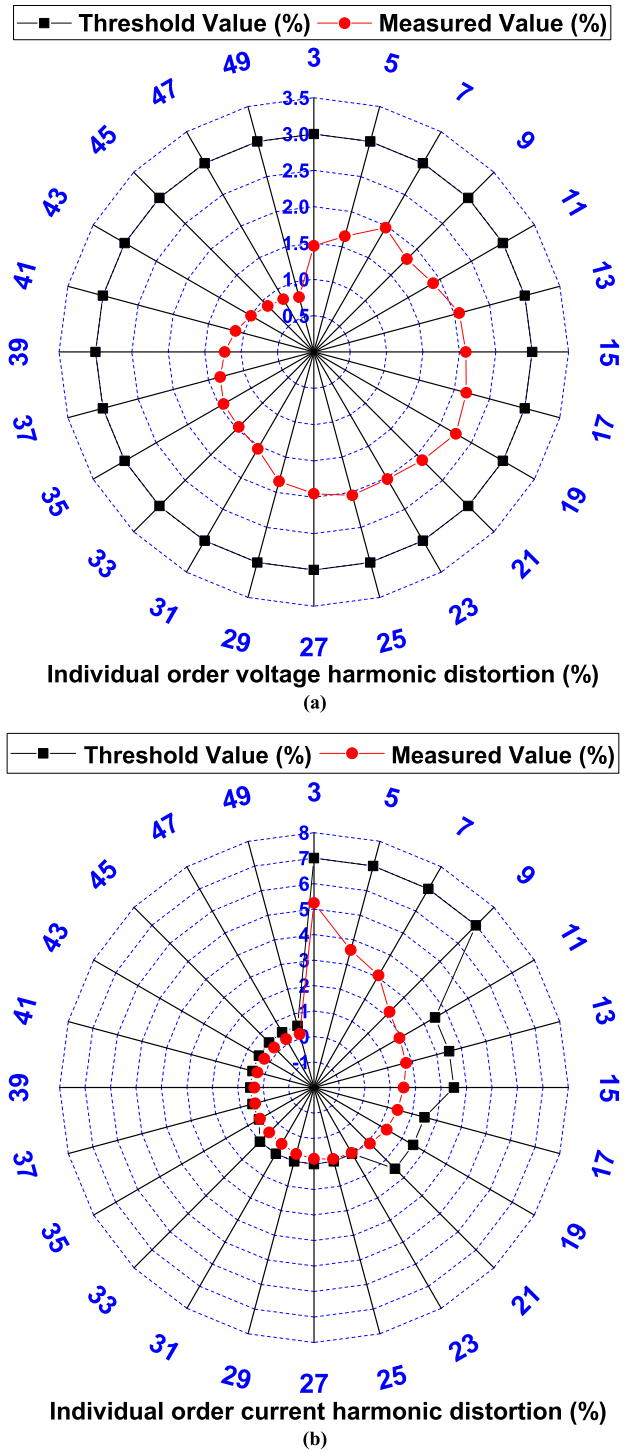

FIGURE 5. (a-b). The radar charts of IHDV and IHDC before compensation.

value stated by IEEE Std. 519 and 1547 respectively in case of with and without DG due to the high level of nonlinearity present in hybrid load. IEEE Std. 1547 suggests that THD of the voltage at the PCC should be below 2.5% for allowing the integration of distributed energy resources and the purpose behind mandating such criterion is to ensure high harmonic constrained HC of the network to be integrated with. Moreover, PF is below the lower threshold value of 0.9 and as a result of the same voltage, the profile is also below 0.95 per-unit. Thus the performance parameters the system without compensation makes it evident that the system does qualify for the need of applying passive filter compensation.

Now it goes obvious that the state of all four objectives (OF_1- OF_4) is miserable in the uncompensated system and impact of the same can be seen on other indices such as voltage profile and transmission losses also because the both improves as the technical and economic benefit of passive filter compensation. For the harmonic distortion reduction and PF improvement in the uncompensated system, high pass filter is designed by the proposed approach keeping the economic consideration of the filter inline simultaneously. The decision variable is defined as $x = (R_f, L_f, C_1, C_2)^T$. The total population of fireflies i.e. 'n' is selected as 30. Total 300 points are generated in Pareto front by running the program 10 times with different, random initial configurations in each run but with the same number of iterations $t = 2,500$. The fixed MOFA parameters are chosen as: $\alpha_0 = 0.25$, $\beta_0 = 1$, $\gamma = 1$. Table 6 shows the control parameter of other three algorithms those are employed for comparative analysis. The proposed algorithm is executed 10 times using MATLAB R2016b. The finally obtained 300 non-dominated individuals are plotted in different 2-axis planes as shown in figure 6. Total 4 plots are obtained by suitable commutation in four OFs to demonstrate the trade-offs among the formulated OFs as well as the actual performance parameters. Each of the planes demonstrates profound optimal design relationships among the objective functions.

Figure 6(a) portrays the Pareto front in the plane of $(OF_1 - OF_2)$ or alternatively portrays the Pareto front of the same in the plane of $(TDD - TVHD)$. According to figure 6(a), low voltage harmonic distortion at the PCC corresponds to low demand distortion in the distribution line while high voltage harmonic distortion at the PCC results in high harmonic current in the distribution line. Figure 6(b) depicts the non-dominated individuals in the plane of $(TDD - FC)$. An almost linear inverse relationship between TDD and the filter cost solution points can be observed in $(3.45 < TDD < 6.8)$ and $(315 < FC < 550)$. It can be concluded that low demand distortion in the distribution line results in the high total cost of the filter while saving in the cost of the filter compromises the power quality in the distribution line. The Pareto front in the plane of $(TVHD - FC)$ and $(PF - FC)$ are shown in figure 6(c) and 6(d) respectively which further indicates that a low-total investment cost corresponds to high voltage-THD. A high total investment cost seems to deliver superior reactive power compensation and harmonic suppression. The trade-off between the two objectives seems rather vague especially in the plane of $(PF - FC)$ but the same can be clearly seen in Pareto front of 2-objective optimization and has been verified by the authors. Figure 6(e) shows the non-dominated individuals in the plane of $(PF - FC)$ obtained by the 2-objective optimization process. It can be seen that figure 6(e) shows a clear trade-off between PF and FC.

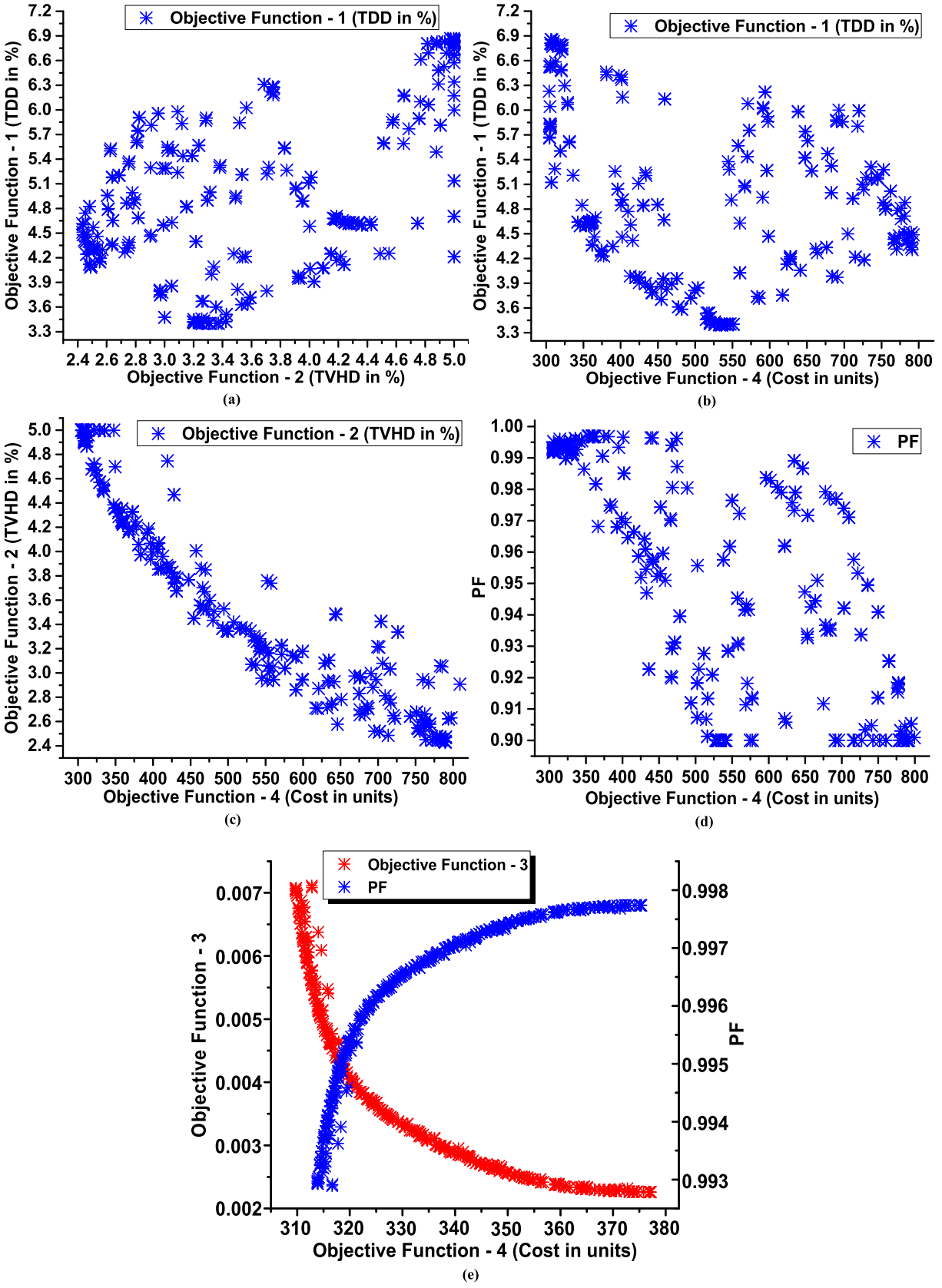

FIGURE 6. (a-e). Final non-dominated solutions obtained by the proposed approach.

TABLE 6. Control parameters of other algorithms.

Parameters	pb-MOPSO [66]	NSGA-II [67]	MOSMA [40]
Number of runs	10	10	10
Population size	30	30	30
Number of iteration	2500	2500	2500
Number of function evaluations	75,000	75,000	75,000
Other related parameters	Personal confidence factor, $c_1 = 1$ Swarm confidence factor, $c_2 = 1$ Inertia weight damping ratio, $W_{damp} = 0.99$ Maximum velocity, $v_{max} = 6$	Crossover probability, $P_c = 0.8$ Mutation probability, $P_m = 0.33$ Cross over index, $\eta_c = 2$ Mutation index, $\eta_m = 20$ Controlled elitism, $r = 0.55$	-

The careful analysis of figure 6(d) shows that the Pareto fronts of figure 6(e) can be seen in this figure and similarly it can be seen for all other planes but all the planes are not included here for the sake of article length. In a generalized way, it can be concluded that the results of 4-objective optimization comprise the Pareto fronts of 2-objective optimization and offer, consequently, more optimal selections to the filter designer.

The obtained Pareto optimal sets reveal also some thought-provoking attributes in terms of design variables. Three different parts can be observed. Some of the objectives are uniformly distributed in all the planes. PF and FC have two parts. One part which is highly populated with corresponding values, $0.993 < PF < 0.998$, $314 < FC < 375$. The corresponding values of objectives for the second part, which is uniformly distributed, can be given as, $0.905 < PF < 0.986$, $345 < FC < 765$. Such facts can be very vital to the filter designer to shift from one optimal solution to another for accomplishing various trade-off necessities of the objectives.

Pareto front obtained by Monte Carlo method is shown in figure 7(a-d). The accuracy and efficiency of the proposed approach, in solving the concerned MOO problem, is validated by comparing three computed performance indices viz. convergence metric, generational distance and diversity metric and the obtained solution with those obtained from two popular multi-objective algorithms namely pb-MOPSO [37], [38], NSGA-II [39] and MOSMA [40]. The Pareto front acquired from Monte Carlo method is approximately considered as the true Pareto front. The definitions of these three performance measures are as follows:

CM and GD measure the distance between the obtained non-dominated front (O_{NDF}) and the Pareto-optimal solutions (P_{Pos}) by using the following equations [63], [64]:

$$CM = \frac{\sum_{i=1}^{|O_{NDF}|} d_i}{|O_{NDF}|} \tag{42}$$

$$GD = \frac{\sqrt{\sum_{i=1}^{|O_{NDF}|} d_i^2}}{|O_{NDF}|} \tag{43}$$

where d_i is the Euclidean distance between the solution $i \in O_{NDF}$ and the nearest number of P_{Pos}.

DM measures the extent of spread achieved among the non-dominated solutions with the following expression [65]:

$$DM = \frac{d_f + d_l + \sum_{i=1}^{|O_{NDF}|-1} |d_i + \bar{d}|}{d_f + d_l + (|O_{NDF}| - 1)\,\bar{d}} \tag{44}$$

where d_i is the Euclidean distance between consecutive solutions in the O_{NDF}, and $\bar{d}$ is the average of these distances. The parameters d_f and d_l represent the Euclidean distance between the extreme solutions of the P_{Pos} and the boundary solutions of the O_{NDF}.

The smaller these performance measures are, the closer the non-dominated solutions are to the TPF. Table 7 shows the comparison of CM, GD and DM of the proposed approach with that of pb-MOPSO, NSGA-II and MOSMA. Table 7 makes it evident that the proposed pb-MOFA based approach provides rather more accurate results than those obtained from PSO, GA and slime mould based approach in terms of GD and DM while MOSMA gives most accurate results in term of CM.

A solution of the proposed method is selected and compared with those obtained by pb-MOPSO, NSGA-II and MOSMA to validate the efficiency of pb-MOFA, in solving the concerned MOO problem.

Table 8 shows the selected solution obtained by the proposed approach versus the solutions obtained by the other two approaches. Table 8 includes also the filter design parameters obtained from the decision vector corresponding to the selected solution out of the total non-dominated set of individuals. Power factor improvement up to 0.9723 is achieved by the proposed approach after trade-off with the total filter cost. While the same is limited to 0.9512, 0.9711 and

TABLE 7. Comparisons USIING convergence metric, generational distance and diversity metric.

Algorithm	Performance Index		
	CM	GD	DM
Proposed	0.0439	0.00761	0.5981
pb-MOPSO	0.0682	0.00798	0.9622
NSGA-II	0.0533	0.00824	0.6851
MOSMA	0.0431	0.00785	0.7114

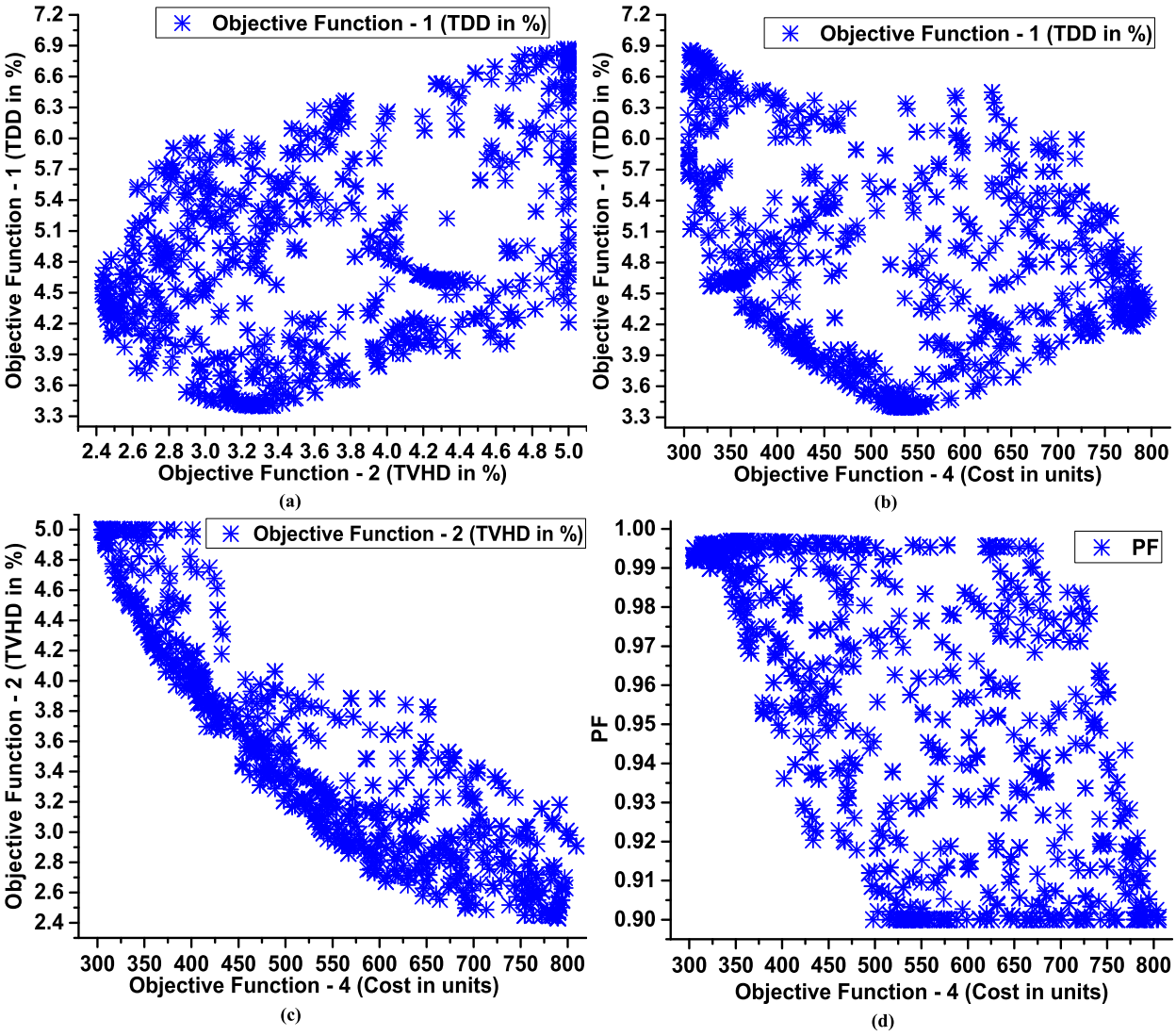

FIGURE 7. (a-d). Pareto front obtained by Monte Carlo method.

0.9568 after simulation with pb-MOPSO, NSGA-II and MOSMA. NSGA-II performs rather better than pb-MOPSO and MOSMA in this regard. The economic benefit of PF improvement can be perceived from transmission losses reducing from 293.81 kW to 213.24 kW. Voltage profile at the PCC is also lying between the lower and upper limit of 0.95 pu and 1.05 pu respectively after the compensation. Though the voltage profile in case of the proposed approach lies much closer to 1 pu yet pb-MOPSO performs marginally better from that aspect and followed by MOSMA. However, the comparison of voltage is little quixotic when the same is not incorporated in the optimization process.

Performance of the system from harmonic distortion aspect can be realised from TVHD as well as TDD as the two indices

TABLE 8. Results of the proposed MOFA based approach versus others.

Parameter	Uncompensated System	Compensated System			
		Proposed	pb-MOPSO	NSGA-II	MOSMA
Filter parameters	**	R_f = 5.98 Ω, L_f = 4.89 mH	R_f = 7.79 Ω, L_f = 5.38 mH	R_f = 6.92 Ω, L_f = 4.28 mH	R_f = 8.32 Ω, L_f = 7.11 mH
	**	C_1 = 136.61 Ω, C_2 = 121.25 mH	C_1 = 185.09 Ω, C_2 = 148.63 mH	C_1 = 138.58 Ω, C_2 = 126.84 mH	C_1 = 136.76 Ω, C_2 = 102.04 mH
	**	h_n = 3.892 m = 0.990	h_n = 2.207 m = 0.479	h_n = 3.321 m = 0.645	h_n = 2.797 m = 0.751
Voltage at the PCC (pu)	0.9329	0.9861	0.9920	0.9862	0.9902
HDF of the distribution line (%)	99.06	99.58	99.60	99.43	99.62
TVHD at the PCC (%)	8.25	3.05	3.07	3.16	3.26
TDD of the line current (%)	7.46	4.63	4.73	5.65	5.01
Transmission losses (kW)	293.81	213.24	221.15	213.93	219.22
PF at the PCC	0.8775	0.9723	0.9512	0.9711	0.9568
Total fundamental power loss in filter (kW)	**	22.09	39.32	22.56	36.78
Filter cost (units)	**	559.87	726.49	580.52	626.68

are under the threshold limit specified by IEEE Std. 519 for all four simulated cases. Moreover, the optimization performance of the proposed MOFA based approach is slightly better than those of pb-MOPSO, NSGA-II and MOSMA. Though pb-MOPSO performs slightly better than NSGA-II and MOSMA in this regard.

The radar charts of IHDV and IHDC are depicted in figure 8. It comprises the same for the proposed one only since there exists an only negligible deviation from the pb-MOPSO, NSGA-II and MOSMA in IHDV and IHDC. In figure 8 only odd-order harmonics are analysed since the same being most detrimental particularly when the nonlinear load spectrum contains only odd-order harmonics in the mainstream [68]. The ampacity of the distribution line is also under the permissible limit with the proposed approach with HDF of 99.58%. The total filter cost incurred, for embroiling the rest three objectives into the system, is also minimum with 559.87 units.

The harmonic filtering performance of the designed filter is assessed by a harmonic attenuation factor. Figure 9 depicts the harmonic attenuation factor and impedance magnitude versus harmonic order for the selected solution. It is observable that there doesn't exist any points with infinite impedances (resonance points) over the entire range of frequencies. Additionally, there are no harmonic currents at the critical point. There is no chance of occurrence of resonance throughout the functioning of the filter since all the harmonic currents are attenuated to very small values.

A. ANALYSIS OF THE IMPACTS OF BVD AND LOAD-SIDE'S NLL ON THE FILTER'S PERFORMANCE

For analysing the impact of BVD and load-side's NLL on the performance of the filter, the system is simulated under (BVD = 1%, NLL = 40%) and (BVD = 4.25%, NLL = 15%). Only odd-order harmonics are considered present in the background since the same is most likely. The international Std., recommends the acceptable limit of BVD is 5%, however practically, such as in many rural oil and gas pumping locations across the US and Canada, it is not exceptional to have more than 5% BVD at the PCC [69]. Moreover, the background voltage at the PCC cannot be controlled as it is virtually not possible to identify what is causing the harmonic voltage distortion. Firstly, while considering the variation of load-side's nonlinearity BVD assumed almost negligible (BVD = 1%) and secondly while taking BVD into consideration (BVD = 4.25%) load is assumed closer to linear (K_n = 15%). Since in the base system, both high nonlinearity level and BVD are considered simultaneously. Table 9 shows the system performance under (BVD = 1%, NLL = 40%) and (BVD = 4.25%, NLL = 15%).

Table 9 shows that, from (BVD = 1%, NLL = 40%) to (BVD = 4.25%, NLL = 40%), TDD drops from 4.84% to 4.63% while TVHD drops from 3.25% to 3.05%. The same variation in BVD also results in a drop of filter cost from 601.36 units to 559.87 units. From (BVD = 4.25%, NLL = 15%) to (BVD = 4.25%, NLL = 40%), TDD hikes from 2.96% to 4.63% while TVHD hikes from 1.92% to 3.05%. The same level of variation in NLL also results in

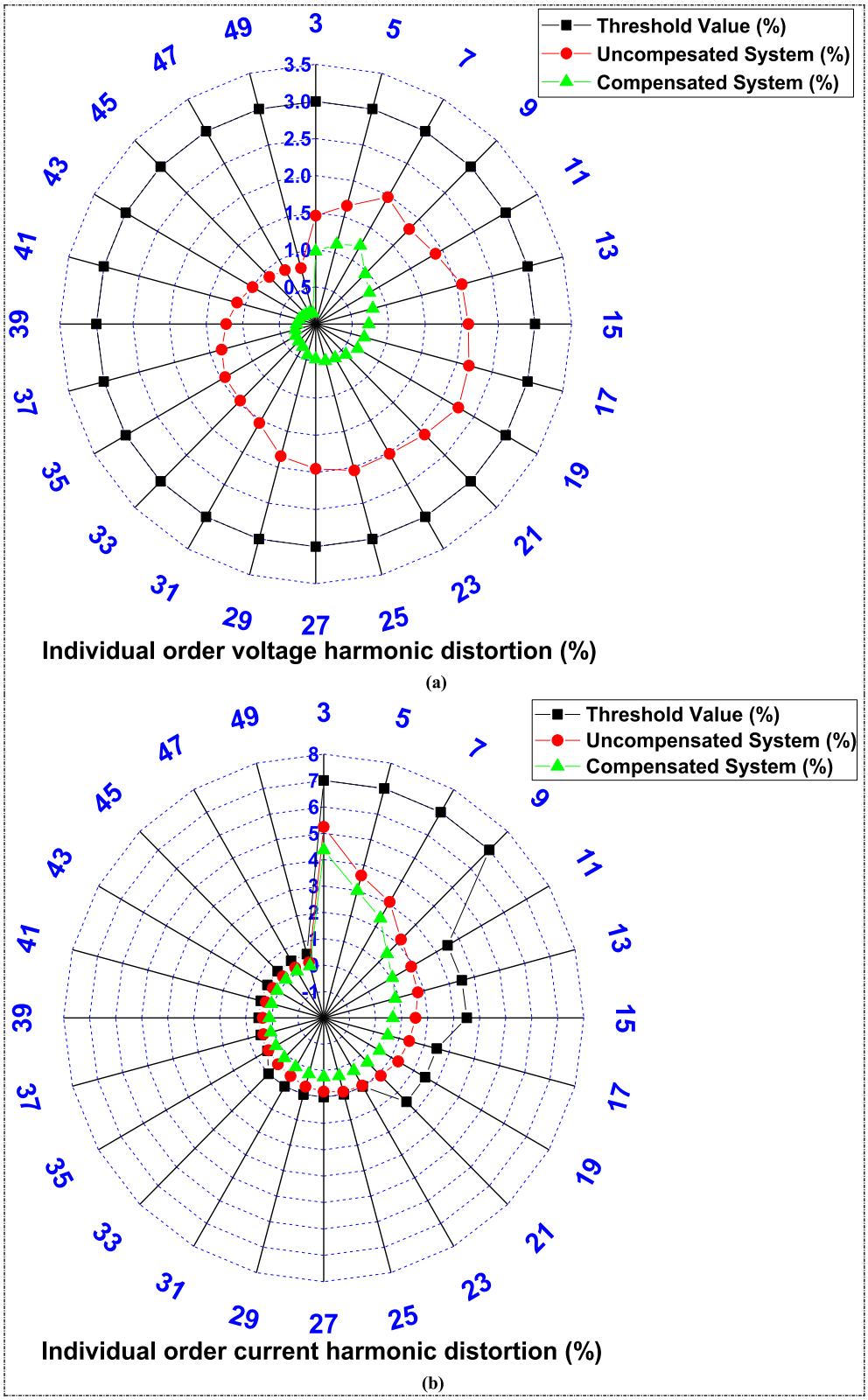

FIGURE 8. (a-b). The radar charts of IHDV and IHDC after compensation.

an increase in filter cost from 371.74 units to 559.87 units. It can be observed that a hike of 3.25% in BVD level results in a partial drop of total filter cost incurred while 25% hike in NLL results in a substantial hike of the same. It is also realized that a hike of 3.25% in BVD level results in partial enhancement of harmonic performance of the system at PCC

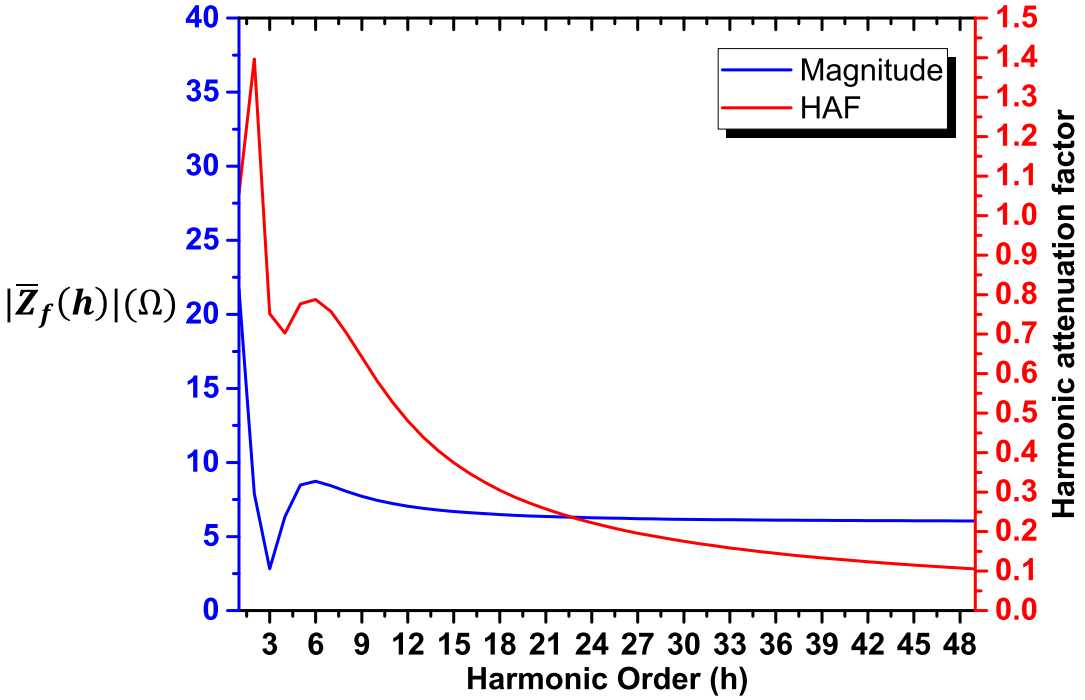

FIGURE 9. Harmonic attenuation factor and impedance magnitude versus harmonic order for the selected solution.

TABLE 9. Results of the proposed approach under two cases.

Parameter	Value	
	Case-1	**Case-2**
	(BVD = 1%, NLL = 40%)	**(BVD = 4.25%, NLL = 15%)**
Filter parameters	R_f = 5.69 Ω, L_f = 4.52 mH	R_f = 10 Ω, L_f = 7.61 mH
	C_1 = 139.20 μF, C_2 = 139.19 μF	C_1 = 113.72 μF, C_2 = 35.46 μF
	h_n = 4.015 m = 0.999	h_n = 2.799 m = 0.669
Voltage at the PCC (pu)	0.9867	0.9768
HDF of the distribution line (%)	99.53	99.81
TVHD at the PCC (%)	3.25	1.92
TDD of the line current (%)	4.84	2.96
Transmission losses (kW)	214.04	207.25
PF at the PCC	0.9702	0.9939
Total fundamental power loss in filter (kW)	25.39	5.38
Filter cost (units)	601.36	371.74

while 25% hike in NLL results in substantial deterioration of the same. The background level at the PCC can be the basis of a significant relationship between the amount of energy that can be generated and the limit for practical purposes and one cannot straightforwardly estimate the DG interconnection limits of a particular system without collecting specific

data on such distortion. Hence, it can be inferred that the presence of background distortion is appreciable from the economic aspect of the filter while the load-side's NLL can be detrimental. From the harmonics mitigation performance perspective, the presence of BVD is still constructive while the load-side's NLL causes a negative impact on the same.

IV. CONCLUSION AND FUTURE DIRECTIONS

In this paper, the optimal passive filter design problem is handled as a multi-objective optimization problem under several constraints of system's performance indices such as harmonic distortion in the line current and PCC's voltage, load power factor, distribution line's ampacity, steady-state voltage profile and a few associated with the filter itself. The optimization problem is formulated as simultaneously determining the accurate design parameters of a third-order damped filter at which PF of the system is maximum while system's other indices such as TDD, TVHD and total FC incurred are minimum by obtaining a best traded-off solution for the system. The multi-objective Pareto-based firefly algorithm has been employed for solving the concerned MOO problem and efficiency as well as the accuracy of pb-MOFA, in solving the concerned MOO problem, is validated by comparing the obtained solution and three computed PIs namely convergence metric, generational distance and diversity metric with those obtained by pb-MOPSO, NSGA-II and MOSMA. The extension of MOFA is considered for producing the Pareto optimal front and the trade-offs among the planned objectives are also analysed by plotting the Pareto optimal fronts on different 2-axis planes. One of the important conclusions drawn from the Pareto fronts is that high filter cost incurs for achieving the high harmonic mitigation and reactive power compensation in the distribution system. The simulation results obtained under various NLL and BVD levels, considered separately infers that the existence of background distortion is advantageous from the economic aspect of the filter while the load-side's NLL can be unfavourable. From the harmonics mitigation performance viewpoint, the presence of BVD is still constructive while the load-side's NLL causes a negative impact on the same.

Since the optimization problem under study is the well-known optimal filter designing problem, therefore, the performance of other metaheuristic optimization algorithms also need to be assessed in this regard in future work. Also, the passive filtering techniques undergo issues in some circumstances such as a change in feeder's impedance and loading level variations. Additionally, it has been proved from the simulation results that the filter's performance is highly dependent on the NLL and BVD levels. Hence there arises the future's need of investigating the active filter solutions for harmonics as well as reactive power compensation and comparing the performance of the two in terms of TDD, TVHD, PF and cost incurred under different NLL and BVD levels because both purely active filter and passive filter supported with small active part (i.e. hybrid active power filter) provide seamless mitigation under high harmonic distortion levels.

REFERENCES

[1] X. Zong, P. A. Gray, and P. W. Lehn, "New metric recommended for IEEE standard 1547 to limit harmonics injected into distorted grids," *IEEE Trans. Power Del.*, vol. 31, no. 3, pp. 963–972, Jun. 2016.
[2] G. K. Singh, "Power system harmonics research: A survey," *Eur. Trans. Electr. Power*, vol. 19, no. 2, pp. 151–172, Mar. 2009.
[3] S. L. Gundebommu, I. Hunko, O. Rubanenko, and V. Kuchanskyy, "Assessment of the power quality in electric networks with wind power plants," in *Proc. IEEE 7th Int. Conf. Energy Smart Syst. (ESS)*, May 2020, pp. 190–194.
[4] *IEEE Standard for Interconnection and Interoperability of Distributed Energy Resources With Associated Electric Power Systems Interfaces*, Institute of Electrical and Electronics Engineers, IEEE Standard 1547-2018, Revision of IEEE Standard 1547-2003, 2018.
[5] *IEEE Recommended Practice and Requirements for Harmonic Control in Electric Power Systems*, IEEE Standard 519-2014 (Revision IEEE Std 519-1992), 2014, pp. 1–29.
[6] M. Bajaj, "Design and simulation of hybrid DG system fed single-phase dynamic voltage restorer for smart grid application," *Smart Sci.*, vol. 8, no. 1, pp. 1–15, Apr. 2020.
[7] S. Kamel, A. Selim, W. Ahmed, and F. Jurado, "Single- and multi-objective optimization for photovoltaic distributed generators implementation in probabilistic power flow algorithm," *Electr. Eng.*, vol. 102, no. 1, pp. 331–347, Mar. 2020.
[8] I. N. Santos, M. H. J. Bollen, and P. F. Ribeiro, "Exploring the concept of hosting capacity for harmonic distortions assessment," in *Proc. IEEE Power Energy Soc. Gen. Meeting*, 2015, pp. 1–5.
[9] S. M. Ismael, S. H. E. Abdel Aleem, A. Y. Abdelaziz, and A. F. Zobaa, "State-of-the-art of hosting capacity in modern power systems with distributed generation," *Renew. Energy*, vol. 130, pp. 1002–1020, Jan. 2019.
[10] A. Singh Rana, M. Bajaj, and S. Gairola, "Optimal power flow solution in smart grid environment using SVC and TCSC," in *Advanced Communication and Control Methods for Future Smartgrids*. Rijeka, Croatia: InTech, 2019, pp. 1–22.
[11] A. Menti, T. Zacharias, and J. Milias-Argitis, "Optimal sizing and limitations of passive filters in the presence of background harmonic distortion," *Electr. Eng.*, vol. 91, no. 2, pp. 89–100, Aug. 2009.
[12] I. F. Mohamed, S. H. E. Abdel Aleem, A. M. Ibrahim, and A. F. Zobaa, "Optimal sizing ofC-type passive filters under non-sinusoidal conditions," *Energy Technol. Policy*, vol. 1, no. 1, pp. 35–44, Jan. 2014.
[13] M. Bajaj and M. Pushkarna, "An IRP based control algorithm for load compensation by DSTATCOM under polluted supply system," in *Proc. Int. Conf. Control Commun. Comput. India (ICCC)*, Nov. 2015, pp. 303–308.
[14] M. Bajaj and A. S. Rana, "Harmonics and reactive power compensation of three phase induction motor drive by photovoltaic-based DSTATCOM," *Smart Sci.*, vol. 6, no. 4, pp. 319–329, Oct. 2018.
[15] G. K. Singh, A. K. Singh, and R. Mitra, "A simple fuzzy logic based robust active power filter for harmonics minimization under random load variation," *Electr. Power Syst. Res.*, vol. 77, no. 8, pp. 1101–1111, Jun. 2007.
[16] B. Singh, V. Verma, A. Chandra, and K. Al-Haddad, "Hybrid filters for power quality improvement," *IEE Proc. Gener., Transmiss. Distrib.*, vol. 152, no. 3, p. 365, 2005.
[17] D. R. Kumar, K. Anuradha, P. Saraswathi, R. Gokaraju, and M. Ramamoorty, "New low cost passive filter configuration for mitigating bus voltage distortions in distribution systems," in *Proc. IEEE Int. Conf. Building Efficiency Sustain. Technol.*, Aug. 2015, pp. 79–84.
[18] J. C. Das, "Passive filters–potentialities and limitations," *IEEE Trans. Ind. Appl.*, vol. 40, no. 1, pp. 232–241, Jan./Feb. 2004.
[19] H. H. Zeineldin and A. F. Zobaa, "Particle swarm optimization of passive filters for industrial plants in distribution networks," *Electr. Power Compon. Syst.*, vol. 39, no. 16, pp. 1795–1808, Oct. 2011.
[20] P. Pinceti and D. Prando, "Sensitivity of parallel harmonic filters to parameters variations," *Int. J. Electr. Power Energy Syst.*, vol. 68, pp. 26–32, Jun. 2015.
[21] T. D. C. Busarello, J. A. Pomilio, and M. G. Simoes, "Passive filter aided by shunt compensators based on the conservative power theory," *IEEE Trans. Ind. Appl.*, vol. 52, no. 4, pp. 3340–3347, Jul. 2016.
[22] H. Na, H. Lina, W. Jian, and X. Dianguo, "Study on optimal design method for passive power filters set at high voltage bus considering many practical aspects," in *Proc. 23rd Annu. IEEE Appl. Power Electron. Conf. Expo.*, Feb. 2008, pp. 396–401.

[23] M. Mohammadi, A. M. Rozbahani, and M. Montazeri, "Multi criteria simultaneous planning of passive filters and distributed generation simultaneously in distribution system considering nonlinear loads with adaptive bacterial foraging optimization approach," *Int. J. Electr. Power Energy Syst.*, vol. 79, pp. 253–262, Jul. 2016.

[24] J. K. Phipps, "A transfer function approach to harmonic filter design," *IEEE Ind. Appl. Mag.*, vol. 3, no. 2, pp. 68–82, 1997.

[25] N. He, D. Xu, and L. Huang, "The application of particle swarm optimization to passive and hybrid active power filter design," *IEEE Trans. Ind. Electron.*, vol. 56, no. 8, pp. 2841–2851, Aug. 2009.

[26] Y.-P. Chang and C.-N. Ko, "A PSO method with nonlinear time-varying evolution based on neural network for design of optimal harmonic filters," *Expert Syst. Appl.*, vol. 36, no. 3, pp. 6809–6816, Apr. 2009.

[27] Y.-M. Chen, "Passive filter design using genetic algorithms," *IEEE Trans. Ind. Electron.*, vol. 50, no. 1, pp. 202–207, Feb. 2003.

[28] S. H. E. Abdel Aleem, A. F. Zobaa, and M. M. Abdel Aziz, "Optimal *C*-type passive filter based on minimization of the voltage harmonic distortion for nonlinear loads," *IEEE Trans. Ind. Electron.*, vol. 59, no. 1, pp. 281–289, Jan. 2012.

[29] G. W. Chang, H.-L. Wang, and S.-Y. Chu, "A probabilistic approach for optimal passive harmonic filter planning," *IEEE Trans. Power Del.*, vol. 22, no. 3, pp. 1790–1798, Jul. 2007.

[30] A. F. Zobaa, "The optimal passive filters to minimize voltage harmonic distortion at a load bus," *IEEE Trans. Power Del.*, vol. 20, no. 2, pp. 1592–1597, Apr. 2005.

[31] Y.-P. Chang and C.-J. Wu, "Optimal multiobjective planning of large-scale passive harmonic filters using hybrid differential evolution method considering parameter and loading uncertainty," *IEEE Trans. Power Del.*, vol. 20, no. 1, pp. 408–416, Jan. 2005.

[32] Z. Xiao-rong, S. Xin-chun, P. Yong-long, and L. He-ming, "Simulated annealing based multi-object optimal planning of passive power filters," in *Proc. IEEE/PES Transmiss. Distrib. Conf. Expo., Asia Pacific*, Aug. 2005, pp. 1–5.

[33] Y.-Y. Hong and C.-S. Chiu, "Passive filter planning using simultaneous perturbation stochastic approximation," *IEEE Trans. Power Del.*, vol. 25, no. 2, pp. 939–946, Apr. 2010.

[34] H. Yassami, S. M. R. Rafiei, G. Griva, A. Dastfan, and A. Darabi, "Multi-objective optimum design of passive filters using SPEA and NSGA-II algorithms," in *Proc. 35th Annu. Conf. IEEE Ind. Electron.*, Nov. 2009, pp. 3679–3685.

[35] Y.-P. Chang, C. Low, and C.-J. Wu, "Optimal design of discrete-value passive harmonic filters using sequential neural-network approximation and orthogonal array," *IEEE Trans. Power Del.*, vol. 22, no. 3, pp. 1813–1821, Jul. 2007.

[36] C.-N. Ko, Y.-P. Chang, and C.-J. Wu, "A PSO method with nonlinear time-varying evolution for optimal design of harmonic filters," *IEEE Trans. Power Syst.*, vol. 24, no. 1, pp. 437–444, Feb. 2009.

[37] A. Stacey, M. Jancic, and I. Grundy, "Particle swarm optimization with mutation," in *Proc. Congr. Evol. Comput. (CEC)*, vol. 2, Dec. 2003, pp. 1425–1430.

[38] C. A. C. Coello, G. T. Pulido, and M. S. Lechuga, "Handling multiple objectives with particle swarm optimization," *IEEE Trans. Evol. Comput.*, vol. 8, no. 3, pp. 256–279, Jun. 2004.

[39] K. Deb, A. Pratap, S. Agarwal, and T. Meyarivan, "A fast and elitist multiobjective genetic algorithm: NSGA-II," *IEEE Trans. Evol. Comput.*, vol. 6, no. 2, pp. 182–197, Apr. 2002.

[40] M. Premkumar, P. Jangir, R. Sowmya, H. H. Alhelou, A. A. Heidari, and H. Chen, "MOSMA: Multi-objective slime mould algorithm based on elitist non-dominated sorting," *IEEE Access*, vol. 9, pp. 3229–3248, 2021.

[41] L. Fusheng, L. Ruisheng, and Z. Fengquan, "Harmonic control of the microgrid," in *Microgrid Technology and Engineering Application*. Amsterdam, The Netherlands: Elsevier, 2016, pp. 137–143.

[42] N.-C. Yang and M.-D. Le, "Optimal design of passive power filters based on multi-objective bat algorithm and Pareto front," *Appl. Soft Comput.*, vol. 35, pp. 257–266, Oct. 2015.

[43] A. F. Zobaa, "Optimal multiobjective design of hybrid active power filters considering a distorted environment," *IEEE Trans. Ind. Electron.*, vol. 61, no. 1, pp. 107–114, Jan. 2014.

[44] S.-J. Jeon, "Non-sinusoidal power theory in a power system having transmission lines with frequency-dependent resistances," *IET Gener., Transmiss. Distrib.*, vol. 1, no. 2, p. 331, 2007.

[45] A. Bonner, T. Grebe, E. Gunther, L. Hopkins, M. B. Man, J. Mahseredjian, N. W. Miller, T. H. Ortmeyer, V. Rajagopalan, S. J. Ranade, P. F. Ribeiro, B. R. Spherling, T. R. Sims, and W. Xu, "Modeling and simulation of the propagation of harmonics in electric power networks. II. Sample systems and examples," *IEEE Trans. Power Del.*, vol. 11, no. 1, pp. 466–474, 1996.

[46] S. H. E. Abdel Aleem, M. E. Balci, and S. Sakar, "Effective utilization of cables and transformers using passive filters for non-linear loads," *Int. J. Electr. Power Energy Syst.*, vol. 71, pp. 344–350, Oct. 2015.

[47] N. Yang and M. Le, "Multi-objective bat algorithm with time-varying inertia weights for optimal design of passive power filters set," *IET Gener., Transmiss. Distrib.*, vol. 9, no. 7, pp. 644–654, Apr. 2015.

[48] T. M. Blooming and D. J. Carnovale, "Application of IEEE STD 519-1992 harmonic limits," in *Proc. Conf. Rec. Annu. Pulp Paper Ind. Tech. Conf.*, 2006 , pp. 1–9.

[49] C.-J. Chou, C.-W. Liu, J.-Y. Lee, and K.-D. Lee, "Optimal planning of large passive-harmonic-filters set at high voltage level," *IEEE Trans. Power Syst.*, vol. 15, no. 1, pp. 433–441, 2000.

[50] A. Hiranandani, "Calculation of cable ampacities including the effects of harmonics," *IEEE Ind. Appl. Mag.*, vol. 4, no. 2, pp. 42–51, 1998.

[51] S. H. E. Abdel Aleem, A. F. Zobaa, and M. E. Balci, "Optimal resonance-free third-order high-pass filters based on minimization of the total cost of the filters using crow search algorithm," *Electr. Power Syst. Res.*, vol. 151, pp. 381–394, Oct. 2017.

[52] W. Xu, T. Ding, X. Li, and H. Liang, "Resonance-free shunt capacitors—Configurations, design methods and comparative analysis," *IEEE Trans. Power Del.*, vol. 31, no. 5, pp. 2287–2295, Jul. 2017.

[53] X. Yang, *Nature-Inspired Metaheuristic Algorithms*. U.K.: Luniver Press, 2008.

[54] I. Fister, I. Fister, X.-S. Yang, and J. Brest, "A comprehensive review of firefly algorithms," *Swarm Evol. Comput.*, vol. 13, pp. 34–46, Dec. 2013.

[55] X. Yang, "Firefly algorithms for multimodal optimization," in *Proc. Int. Symp. Stochastic Algorithms*, 2009, pp. 169–178.

[56] P. Lezhniuk, V. Teptya, V. Komar, and O. Rubanenko, "Principle of least action in models and algorithms of optimisation states power system," *Model., Control Inf. Technol.*, no. 3, pp. 173–176, Nov. 2019.

[57] K. Nadhir, D. Chabane, and B. Tarek, "Distributed generation location and size determination to reduce power losses of a distribution feeder by firefly algorithm," *Int. J. Adv. Sci. Technol.*, vol. 56, pp. 61–72, Jul. 2013.

[58] M. H. Sulaiman, M. W. Mustafa, A. Azmi, O. Aliman, and S. R. A. Rahim, "Optimal allocation and sizing of distributed generation in distribution system via firefly algorithm," in *Proc. IEEE Int. Power Eng. Optim. Conf.*, Jun. 2012, pp. 84–89.

[59] S. Saravanamutthukumaran and N. Kumarappan, "Sizing and siting of Distribution Generator for different loads using firefly algorithm," in *Proc. IEEE-Int. Conf. Adv. Eng. Sci. Manag. (ICAESM)*, Mar. 2012, pp. 800–803.

[60] X.-S. Yang, "Multiobjective firefly algorithm for continuous optimization," *Eng. Comput.*, vol. 29, no. 2, pp. 175–184, Apr. 2013.

[61] M. Yan Kit, W. H. Lau, and C. F. N. Tse, "A study on the effects of voltage distortion on current harmonics generated by modern SMPS driven home appliances in smart grid network," in *Proc. 9th IET Int. Conf. Adv. Power Syst. Control, Operation Manage. (APSCOM)*, 2012, p. 85.

[62] M. Bajaj, S. Rautela, and A. Sharma, "A comparative analysis of control techniques of SAPF under source side disturbance," in *Proc. Int. Conf. Circuit, Power Comput. Technol. (ICCPCT)*, Mar. 2016, pp. 1–7.

[63] M. Laszczyk and P. B. Myszkowski, "Survey of quality measures for multi-objective optimization: Construction of complementary set of multi-objective quality measures," *Swarm Evol. Comput.*, vol. 48, pp. 109–133, Aug. 2019.

[64] A. Unveren and A. Acan, "Multi-objective optimization with cross entropy method: Stochastic learning with clustered Pareto fronts," in *Proc. IEEE Congr. Evol. Comput.*, 2007, pp. 3065–3071.

[65] N. Riquelme, C. Von Lucken, and B. Baran, "Performance metrics in multi-objective optimization," in *Proc. Latin Amer. Comput. Conf. (CLEI)*, Oct. 2015, pp. 1–11.

[66] H. Borhanazad, S. Mekhilef, V. Gounder Ganapathy, M. Modiri-Delshad, and A. Mirtaheri, "Optimization of micro-grid system using MOPSO," *Renew. Energy*, vol. 71, pp. 295–306, Nov. 2014.

[67] P. Murugan, S. Kannan, and S. Baskar, "NSGA-II algorithm for multi-objective generation expansion planning problem," *Electr. Power Syst. Res.*, vol. 79, no. 4, pp. 622–628, Apr. 2009.

[68] M. S. K. Dartawan, R. Austria, and L. Hui, "Harmonics issues that limit solar photovoltaic," in *Proc. World Renew. Energy Forum (WREF)*. Denver, CO, USA: Colorado Convention Centre, 2012, pp. 1–7.
[69] I. Wallace, A. Bendre, and N. Wood, "Harmonic filters for Hogh background voltage distortion applications," TCI, LLC, Washington, DC, USA, Tech. Pap., 2013, pp. 1–5.

MOHIT BAJAJ (Member, IEEE) was born in Roorkee, India, in 1988. He received the bachelor's degree in electrical engineering from the FET, Gurukula Kangri Vishwavidhyalya, Haridwar, India, in 2010, and the M.Tech. degree in power electronics and ASIC design from NIT Allahabad, India, in 2013. He is currently pursuing the Ph.D. degree with the Department of Electrical and Electronics Engineering, NIT Delhi, India. He has academic experience of five years. He has published over 30 research papers in reputed journals, international conferences, and book chapters. His research interests include power quality improvement in renewable DG systems, distributed generations planning, application of multi-criteria decision making in power systems, custom power devices, the IoT, and smart grids. He is also a member of PES.

NAVEEN KUMAR SHARMA (Member, IEEE) received the B.Tech. degree in electrical and electronics engineering from Uttar Pradesh Technical University Lucknow, in 2008, and the M.Tech. and Ph.D. degrees in power system from the National Institute of Technology Hamirpur, India, in 2010 and 2014, respectively. He worked as a Lecturer with the Department of Electrical Engineering, National Institute of Technology Hamirpur, from March 2014 to May 2017. He is currently an Assistant Professor with the Department of Electrical Engineering, I. K. G. Punjab Technical University, Kapurthala. He has published several research papers in leading international journals and conference proceedings, and presented papers at several prestigious academic conferences, such as IEEE and Springer. His research interests include power market, renewable energy sources, power system optimization, and condition monitoring of transformers.

MUKESH PUSHKARNA was born in Roorkee, India, in 1988. He received the bachelor's degree in electrical engineering from the FET, Gurukula Kangri Vishwavidhyalya, Haridwar, India, in 2010, and the M.Tech. degree in power system and management from Jamia Millia Islamia University, New Delhi, India, in 2013, where he is currently pursuing the Ph.D. degree with the Department of Electrical and Electronics Engineering. He is also working as an Assistant Professor with GLA University Mathura, India. He has academic experience of five years. His research interests include power quality improvement in renewable DG systems, distributed generations planning, power systems, and smart grids.

HASMAT MALIK (Senior Member, IEEE) received the M.Tech. degree in electrical engineering from the National Institute of Technology (NIT) Hamirpur, India, and the Ph.D. degree in electrical engineering from the Indian Institute of Technology (IIT), Delhi. He has been a Research Fellow with BEARS, University Town, NUS Campus, Singapore, since January 2019. He has served as an Assistant Professor for five years at the Division of Instrumentation and Control Engineering, Netaji Subhas Institute of Technology (NSIT), Delhi, India. He is currently a Chartered Engineer and a Professional Engineer. He organized five international conferences, and proceedings have been published by Springer Nature. He has published widely in international journals and conferences his research findings related to Intelligent Data Analytic, Artificial Intelligence, Machine Learning Applications in Power System, Power Apparatus, Smart Building & Automation, Smart Grid, Forecasting, and Prediction and Renewable Energy Sources. He has authored/coauthored more than 100 research articles and eight books and 13 chapters in nine other books, published by IEEE, Springer, and Elsevier. He has supervised 23 PG students. He is involving in several large research and development projects. His research interests include artificial intelligence, machine learning and big-data analytics for renewable energy, smart building and automation, condition monitoring, and online fault detection and diagnosis (FDD). He is also a Life Member of Indian Society for Technical Education (ISTE), Institution of Electronics and Telecommunication Engineering (IETE), International Society for Research and Development (ISRD), London, Computer Science Teachers Association (CSTA), USA, Association for Computing Machinery (ACM) EIG, and Mir Labs, Asia. He received the POSOCO Power System Award (PPSA-2017) for his Ph.D. work for research and innovation in the area of power system. He also received best research papers awards at IEEE INDICON-2015, and full registration fee award at IEEE SSD-2012 (Germany).

MAJED A. ALOTAIBI (Member, IEEE) received the B.Sc. degree in electrical engineering from King Saud University, Riyadh, Saudi Arabia, in 2010, and the M.A.Sc. and Ph.D. degrees in electrical and computer engineering from the University of Waterloo, Waterloo, ON, Canada, in 2014 and 2018, respectively. He worked as an Electrical Design Engineer with ABB Saudi Arabia. He is currently an Assistant Professor with the Department of Electrical Engineering, King Saud University, and the Director of Saudi Electricity Company Chair for Power System Reliability and Security. He is also serving as the Vice Dean for academic affairs at the College of Engineering, King Saud University. His research interests include power system planning, operation, renewable energy modeling, applied optimization, and smart grid. He has served as a Reviewer for the IEEE TRANSACTIONS ON POWER SYSTEMS and the IEEE TRANSACTIONS ON SMART GRIDS.

ABDULAZIZ ALMUTAIRI (Member, IEEE) received the B.Sc. degree in electrical engineering from Qassim University, Buraydah, Saudi Arabia, in 2009, and the M.A.Sc. and Ph.D. degrees in electrical and computer engineering from the University of Waterloo, Waterloo, ON, Canada, in 2014 and 2018, respectively. He is currently an Assistant Professor with the Electrical Department, Majmaah University, Saudi Arabia. His research involves both experimental studies and modelling of many system problems. His research interests include asset management in smart grids, power system reliability and resilience, and development of innovating techniques for integrating renewable energy resources and electric vehicle to power systems.